Charles University in Prague
Faculty of Science

Department of Cell Biology

Phenotype analysis of *Schizosaccharomyces pombe* strains harbouring deletions of the *cbf11* and *cbf12* genes

Diploma Thesis

Jana Staňurová

2009

Supervised by Mgr. Martin Převorovský, Ph.D.

I hereby declare that this submission is my own work and that, to the best of my knowledge and belief, it contains no material previously published or written by another person nor material which to a substantial extent has been accepted for the award of any other degree or diploma of the university or other institute of higher learning, except where due acknowledgment has been made in the text.

Prague, May 2009 Jana Staňurová

ACKNOWLEDGEMENTS

In the first place I wish to express my gratitude to my supervisor Mgr. Martin Převorovský, Ph.D., for his guidance, patience, advice and support through these years and for always being there when I needed it. I also want to thank the other members of our laboratory, especially to my team-colleague Martina Ptáčková, for their help.

My very special thanks belong to my family and my dear friends for their love, care and support, for believing in me, comforting me whenever I struggled and always being there for me. You made it possible.

TABLE OF CONTENTS

ABBREVIATIONS

5Tm	5 transmembrane passes
BTD	beta-trefoil domain
CBF1	C-promoter binding factor 1
CD	circular dichroism
CSL	CBF1/RBP-Jκ/Suppressor of Hairless/LAG-1
C_T	threshold cycle
DAPI	4',6-diamidino-2-phenylindole
DABCO	1,4-diazabicyclo[2.2.2]octane
DSL	Delta/Serrate/LAG-2
ECL	enhanced chemiluminescence
EDTA	ethylene diamine tetraacetic acid
EGTA	ethylene glycol tetraacetic acid
FACS	fluorescence-assisted cell sorter
HEPES	4-(2-hydroxyethyl)-1-piperazineethanesulfonic acid
LAG-1/2/3	lin-12 and glp-1 signaling
NAD^+	nicotinamide adenine dinucleotide
NICD	Notch intracellular domain
ORF	open reading frame
PAGE	polyacrylamide gel electrophoresis
PCR	polymerase chain reaction
PIPES	piperazine-1,4-bis(2-ethanesulfonic acid)
qPCR	quantitative real-time polymerase chain reaction
qRT-PCR	quantitative real-time reverse transcription-polymerase chain reaction
RBP-Jκ	recombination signal binding protein Jκ
RBP-L	RBP-Jκ-like
RHR	Rel-homology region
SDS	sodium dodecyl sulphate

1 *INTRODUCTION*

Schizosaccharomyces pombe, also known as fission yeast, is a simple unicellular eukaryotic model organism. Phylogenetically belonging to Taphrinomycotina (Hedges, 2002), it is a distant cousin of budding yeast, *Saccharomyces cerevisiae*, although its various molecular and cellular processes and characteristics resemble higher eukaryotes more closely, thus making fission yeast a preferable model for studying the cell cycle, polarity, chromatin organisation and gene expression (Egel, 2004). Genome of *Schizosaccharomyces pombe* has already been completely sequenced and harbours approximately 5000 genes (Wood *et al.*, 2002).

Recently, two novel members of the CSL family of transcription factors have been identified in *Schizosaccharomyces pombe* (Prevorovsky *et al.*, 2007). The CSL family (CBF1/RBP-Jκ/Suppressor of Hairless/LAG-1), previously considered to be merely metazoan, are engaged in the Notch signalling pathway, thus being involved in key developmental processes (Artavanis-Tsakonas *et al.*, 1999). Therefore, the existence of CSL genes in fungal organisms is all the more evolutionarily interesting, as Notch signalling is not present there.

One of the classical methods to determine functions of a gene is creation of a mutant strain bearing deletion of the gene, and its successive analysis. The aim of the study described in this thesis is to phenotypically characterise such strains of *Schizosaccharomyces pombe*, which lack the genes coding for the two respective members of CSL family, and, by these means, to assess their roles in this fungal organism.

2 *LITERATURE REVIEW*

2.1 CSL proteins

Named after three members identified in mammals, *Drosophila melanogaster* and *Caenorhabditis elegans* (CBF1/RBP-Jκ/Suppressor of Hairless/LAG-1) the CSL proteins serve as transcription factors, in both activating and repressive manner, depending on context. Their functions have been best described as the effector element of Notch signalling pathway (Bray and Furriols, 2001; Lai, 2002; Pursglove and Mackay, 2005), which is a critical regulatory cascade implicated in mediating many developmental events in metazoa (Artavanis-Tsakonas, 1999). Notch is a large single-pass transmembrane receptor protein situated on the cell surface. During maturation the receptor is cleaved and the proteolytic fragments form a non-covalent heterodimer consisting of a large extracellular domain attached to a transmembrane part that extends into the cell cytoplasm, forming the Notch intracellular domain, NICD (see Figure 2.1). The receptor recognises ligands of the Delta/Serrate/LAG-2 type (DSL; abbreviation formed from the mammalian, *Drosophila melanogaster* and *Caenorhabditis elegans* orthologs) which also are transmembrane proteins, thus permitting only short distance cell-cell signalling via this pathway (see Figure 2.1). Upon ligand binding, two sequential proteolytic events take place liberating the NICD, which then translocates to the cell nucleus to exert its coactivator function at target promoters. Interestingly, no second messengers amplify the signal. In the nucleus, NICD interacts with the third component, a DNA-bound transcription factor of the CSL family, an effector protein which in turn switches from a repressive mode by displacement of corepressors to an activatory state upon recruitment of Mastermind and other coactivators (see Figure 2.1). The principal aim of the signalling is promotion or inhibition of a particular cell fate, such as lateral inhibition, cell lineage decision or boundary specification. The signalling outcome is highly context-dependent and is a subject to complex regulation by both the ligand and receptor expression levels and turnover, their localisation pattern, and posttranslational modifications (Bray, 2006). However, the involvement of CSL family members was found not to be restricted to the Notch framework only (Barolo, 2000; Koelzer and Klein, 2003; Masui, 2007).

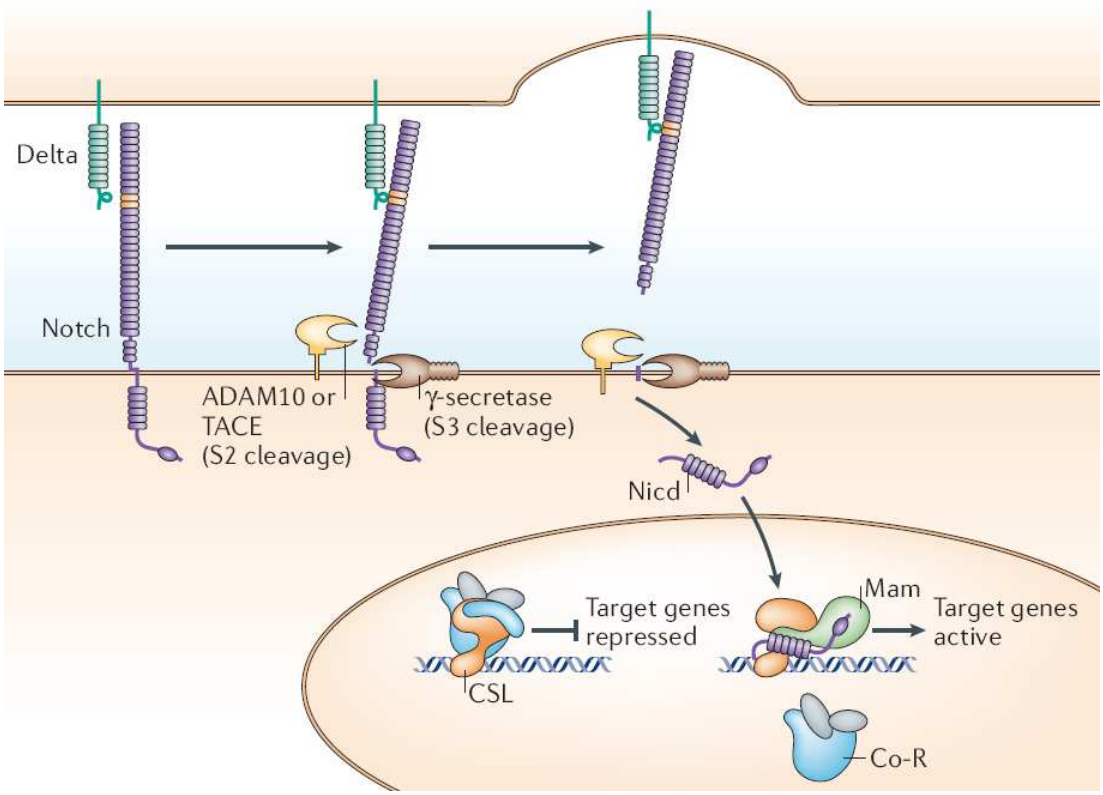

Figure 2.1 – A schematic representation of the Notch signalling pathway, see text for details (adapted from (Bray, 2006)). Co-R – corepressor complex; Mam – Mastermind.

2.1.1 CSL family phylogeny

Until recently, the presence of CSL genes in the genome was considered a hallmark of metazoan organisms, especially concerning their association with developmental processes (Weinmaster and Kintner, 2003). However, members of the CSL protein family have been predicted, identified and described in fungi as well (Prevorovsky *et al.*, 2007; Prevorovsky *et al.*, 2008). A wide range of organisms harbour CSL family representatives, whose degree of conservation across evolution was proven surprisingly high, being prominent in the DNA binding region (Kovall and Hendrickson, 2004; Prevorovsky *et al.*, 2007; Prevorovsky *et al.*, 2008).

Interestingly, most vertebrates have two paralogs of the CSL genes, one of which is engaged in the Notch pathway (CBF1/RBP-Jκ) and has been rather well characterised unlike the other paralog, RBP-L (stands for RBP-Jκ-like). The latter manifests lower degree of conservation and its expression is only confined to some organs or tissues. Furthermore, this paralog seems to function in a manner independent of the Notch pathway (Beres *et al.*, 2006; Minoguchi *et al.*, 1997), e.g. in the development of pancreas (Masui *et al.*, 2007).

2.1.2 CSL protein structure

The crystal structures of the DNA-bound CSL proteins from *Caenorhabditis elegans* and human were recently prepared (Kovall and Hendrickson, 2004; Wilson and Kovall, 2006). The protein structure consists of three distinct domains, each of which is similar to known structures. As suggested by structural comparison, the CSL protein fold is globally similar to Rel proteins. The C-terminal domain resembles an IPT/TIG domain, RHR-C (Rel-homology region-C) and the N-terminal domain is similar to an RHR-N domain. Surprisingly, in the place of a virtual junction between the two domains of a Rel protein, there is a beta-trefoil domain (BTD) situated in the CSL protein. The BTD region includes a long β-strand linker that interconnects the three domains by contributing to β-sheets present in all of them, thus being the key organising feature of the whole CSL protein (see Figure 2.2).

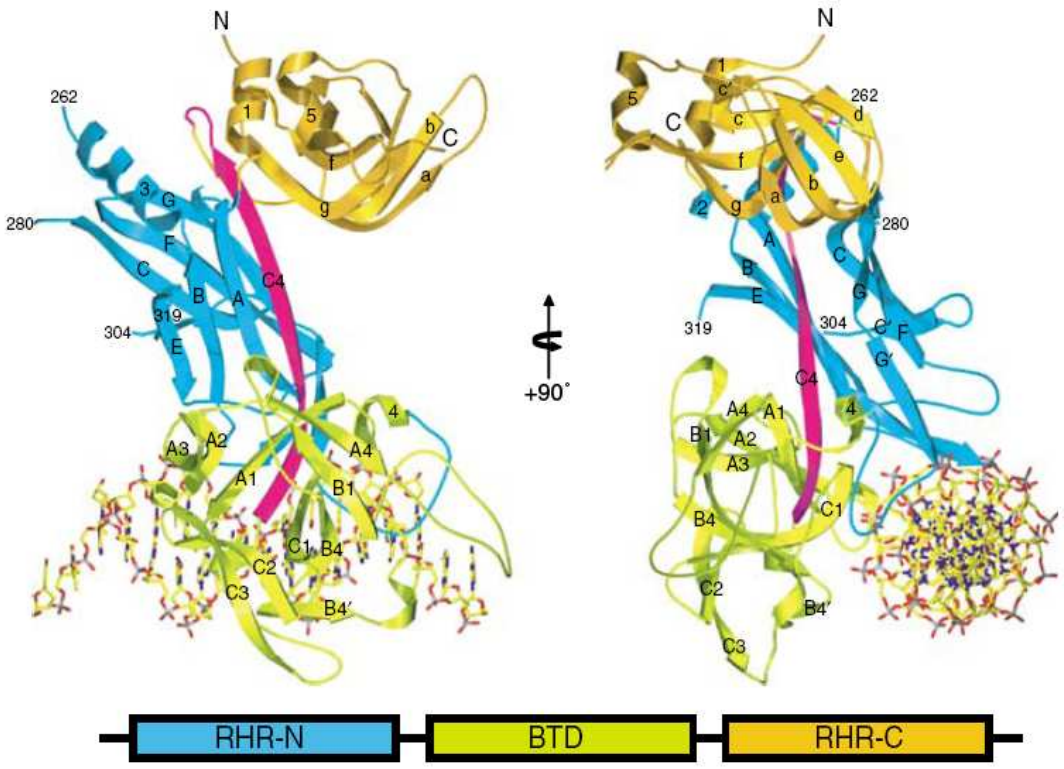

Figure 2.2 – Ribbon representation of the *Caenorhabditis elegans* CSL–DNA complex and domain organisation. Orthogonal views are shown. A schematic representation of the domain arrangement is also shown (adapted from (Kovall and Hendrickson, 2004)).

RHR-N, BTD and a part of the long β-strand linker are responsible for binding to DNA. Detailed mapping was performed for the known binding sites of various interaction partners (both coactivators and corepressors) and most of them cluster to and around a conserved hydrophobic pocket on BTD. However, further interactions of NICD and Mastermind with RHR-C were found (Kovall, 2007). Significantly, the regions of the CSL proteins being most conserved throughout evolution are those involved in DNA binding (see Figure 2.3).

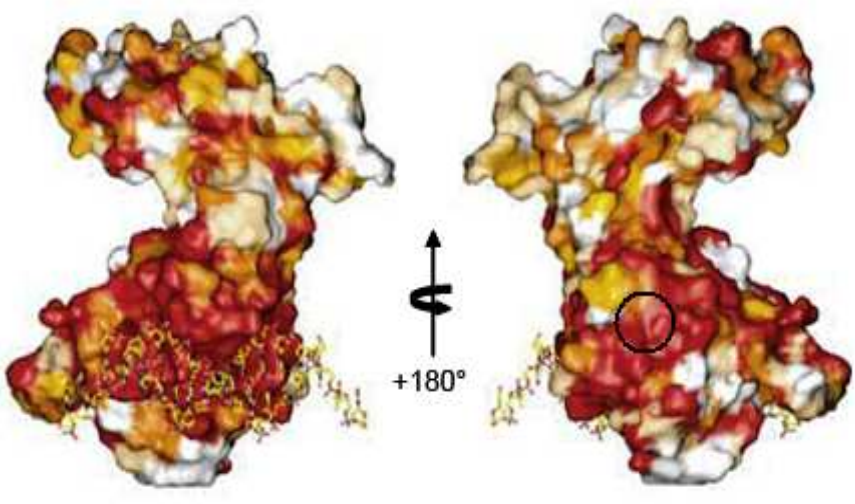

Figure 2.3 – CSL sequence conservation mapped to the molecular surface. Dark red, orange, yellow, and white represent regions of absolute identity, high and moderate similarity, and regions of no conservation, respectively. The protein–DNA interface is entirely conserved. The hydrophobic pocket (circle) is also highly conserved (adapted from (Kovall and Hendrickson, 2004)).

2.1.3 DNA binding properties

CSL proteins were identified as factors binding to the immunoglobulin Jκ recombination signal sequence (recombination signal binding protein RBP-Jκ) consisting of a conserved heptamer CACTGTG and an A/T-rich nonamer separated by a spacer of 23 bp (Hamaguchi *et al.*, 1989). Later, the reported CSL binding preference for the Jκ recombination signal was proved an artefact caused by introduction of a *Bam*HI site next to the heptamer sequence resulting in the appearance of a suboptimal CSL-binding site cactGTG+GGAtcc (Henkel *et al.*, 1994; Honjo, 1996; Matsunami *et al.*, 1989). Additional extensive analysis of the CSL protein DNA-binding properties rendered the GTG(G/A)GAA canonical response element as it is known at present and a number of non-canonical sites with

a higher or lower degree of variance, such as TGGGAAA, TGGGAAAGAA or CATGGGAA (Morel and Schweisguth, 2000; Shirakata *et al.*, 1996; Tun *et al.*, 1994). Mammalian RBP-L paralog seems to have cognate target site specificity (Beres *et al.*, 2006). Although murine RBP-Jκ protein was found to bind DNA as a monomer (Chung *et al.*, 1994), recent data indicate the possibility of cooperative binding with other factors. It is noteworthy that the mammalian RBP-Jκ family member was identified in an independent study as CBF1, a protein binding to the C promoter in the Epstein-Barr virus genome (Henkel *et al.*, 1994). Therefore, concerning the above stated facts, the CBF1 denomination should be used.

2.1.4 CSL proteins in fungi

As stated above, members of the CSL family have recently been predicted and identified in fungi (Prevorovsky *et al.*, 2007; Prevorovsky *et al.*, 2008). Their presence in the kingdom of fungi is all the more interesting from the evolution point of view, since the Notch signalling pathways is not present, the notorious metazoan interaction partners are not present either, and, obviously, the embryonic development is absent. However, the overall protein structure remains conserved among species (see Figure 2.5 for comparison) and the DNA binding regions display absolute sequence conservation (see Figure 2.3 and Figure 2.4).

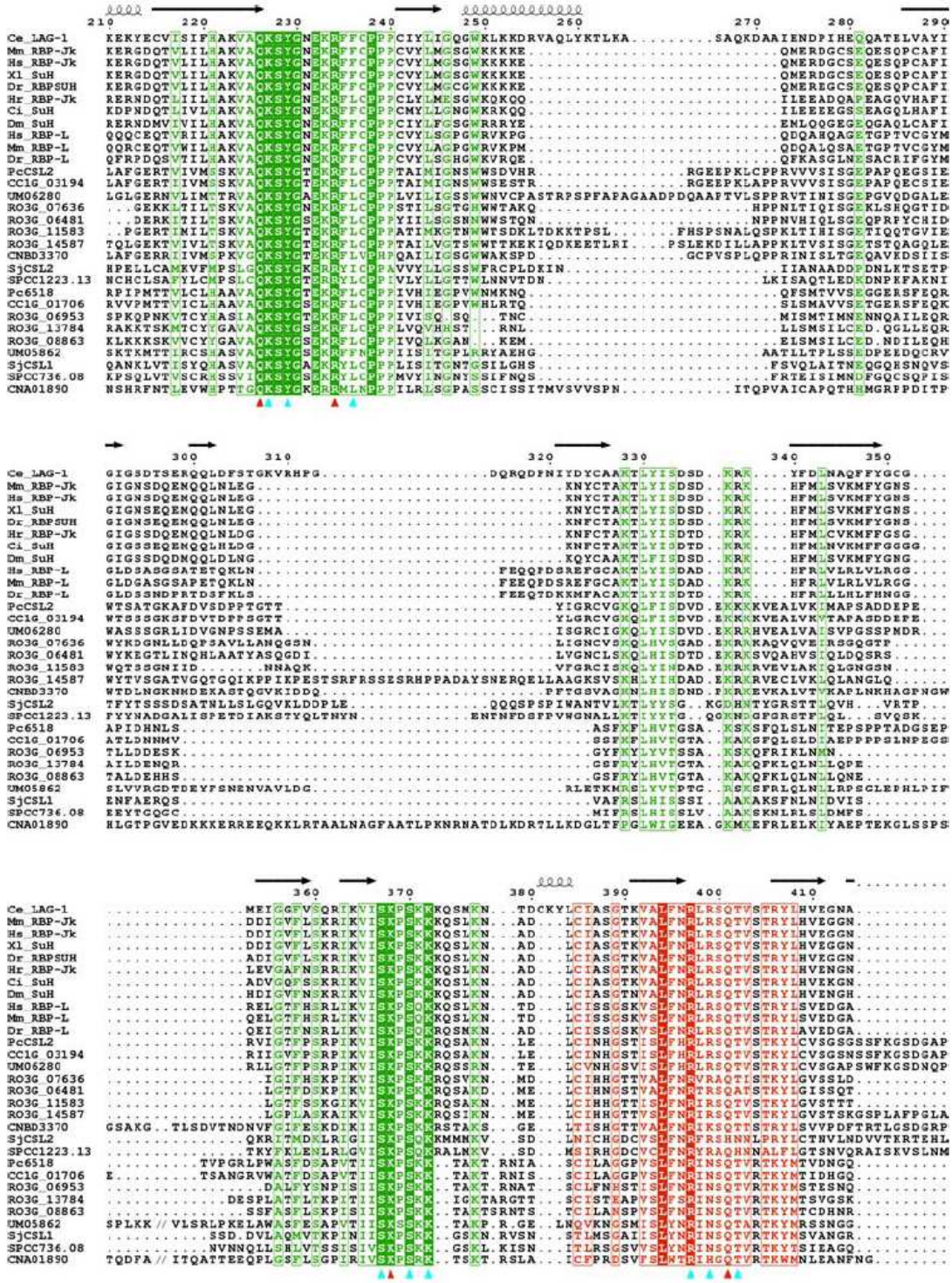

Figure 2.4a – Evolutionary conservation of the DNA-binding regions. The alignment of fungal and selected metazoan CSL protein sequences shows high degree of conservation in regions responsible for DNA binding. Absolutely conserved residues are inverse-printed, positions with high residue similarity are boxed. Domain boundaries are indicated by colour: green for RHR-N, red for BTD and blue for the β-strand linker connecting all three CSL domains. Red and cyan triangles below the alignment denote residues required for sequence specific and backbone DNA binding, respectively. The position numbering and secondary structures indicated above the sequences correspond to

Caenorhabditis elegans LAG-1 (Kovall and Hendrickson, 2004). The picture shows only a selected region of the whole alignment and, in order to save space, some parts of the long inserts are not shown (indicated by '//'). The picture was taken from (Prevorovsky *et al.*, 2007).

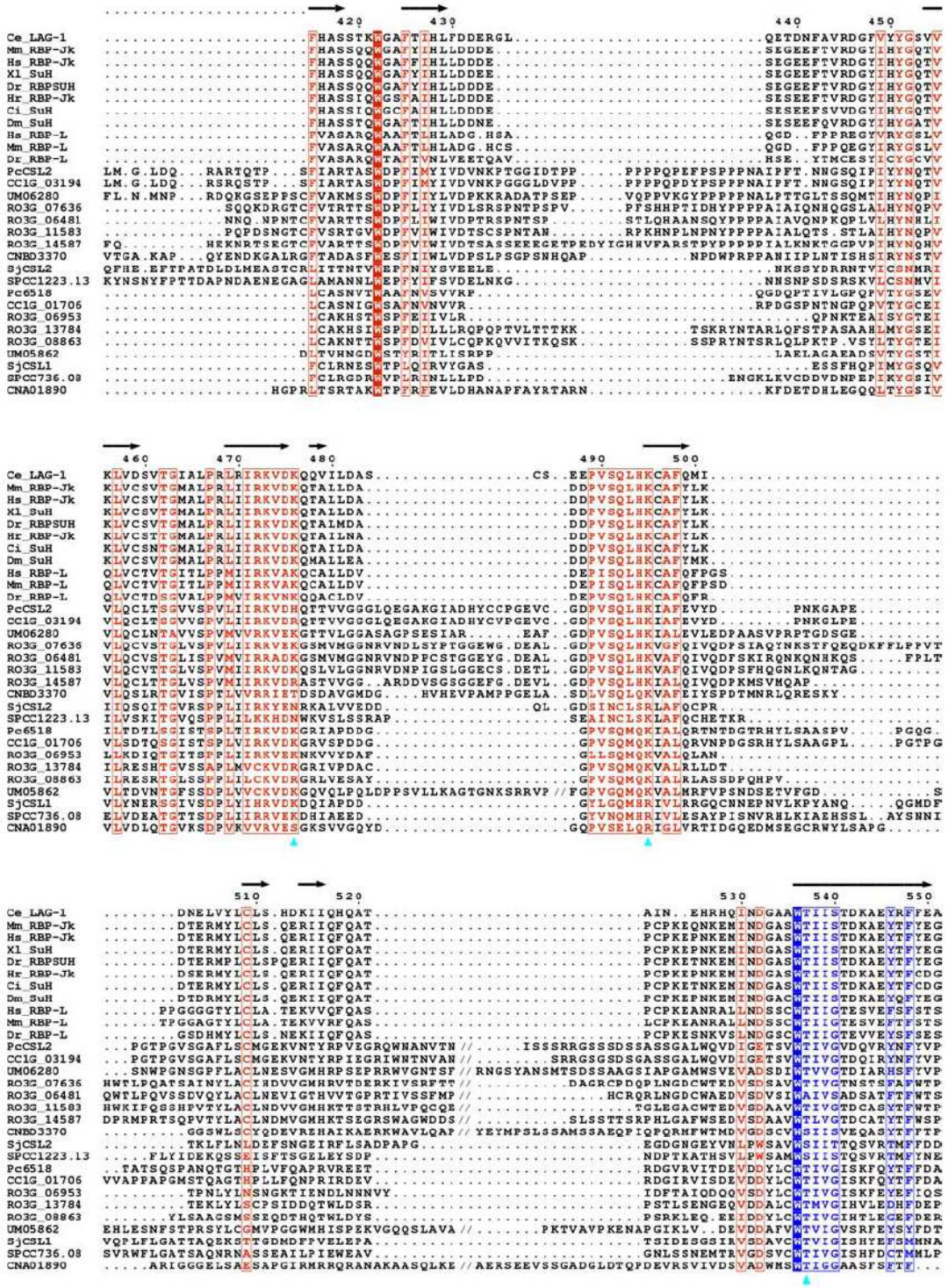

Figure 2.4b – Evolutionary conservation of the DNA-binding regions, continued. The picture was taken from (Prevorovsky *et al.*, 2007).

Two CSL family paralogs were described in *Schizosaccharomyces pombe*, namely Cbf11 and Cbf12 (Prevorovsky *et al.*, 2007; Prevorovsky *et al.*, 2008). The latter had been predicted nuclear; the former had been predicted exclusively non-nuclear. However, Cbf11 too was experimentally proved to localise to the nucleus (Prevorovsky *et al.*, 2008), supporting the hypothesis for both proteins being transcription factors. In comparison with the metazoan members of CSL family the N-terminal sequences of both Cbf11 and Cbf12 are rather prolonged. While the DNA binding properties of Cbf11 resemble those of the metazoan othologs, such characteristics for Cbf12 have not been determined to a satisfactory degree and remain yet to be specified.

Cbf11 is 613 amino acid residues long and is constitutively expressed throughout the phases of the cell cycle. On the contrary, the 963 amino acid residues long Cbf12 seems to be differentially expressed. Its expression rate is elevated upon the entry to stationary phase and also meiosis (Prevorovsky *et al.*, 2008).

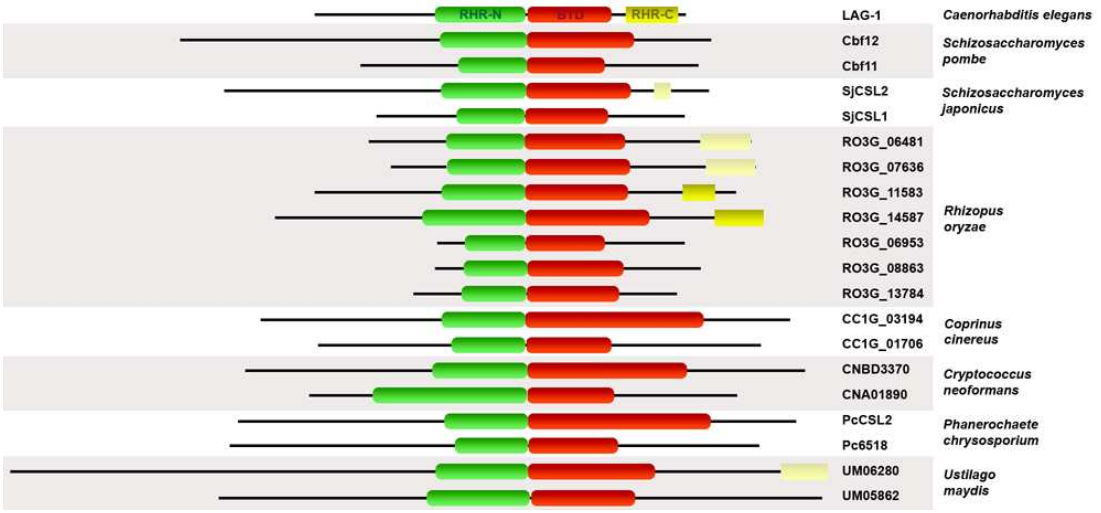

Figure 2.5 – Fungal CSL proteins domain organisation. Black lines represent the respective CSL protein sequences. The structure of *Caenorhabditis elegans* LAG-1 is shown at the top for comparison (Kovall and Hendrickson, 2004). Recognized Pfam domains are indicated: RHR-N in green, BTD in red and RHR-C in yellow (light yellow for low significance). The proteins are drawn to scale (adapted from (Prevorovsky *et al.*, 2007)).

2.2 Adhesion properties in yeast

Yeast cells possess a capacity to adhere to surfaces, other cells and tissues, which is critical for development, symbiosis and pathogenesis. Adhesion or flocculation (formation of macroscopic cell aggregates, named flocs, in liquid medium) are conferred by special cell wall proteins called adhesins and are triggered in response to stress, nutrient starvation or small molecules produced by neighbouring cells or host organisms. Upon activation of the adhesin genes fungi can adhere to substrates and penetrate them in order to find new nutrients (Gagiano *et al.*, 2002; Kron, 1997). Flocculation may provide protection from environmental stresses to the cells situated in the middle of the flocs. Moreover, either the flocs sediment in the liquid medium, or they float to the surface; in other words, escape from the stress inducing factors. Cells are equipped with different adhesins which allow for adhesion to specific substrates. Cell adhesion proteins are crucial in mating, colony morphology changes, biofilm establishment and interaction with hosts. Adhesins are subject to subtelomeric epigenetic switching (De Las Penas *et al.*, 2003; Domerque *et al.*, 2005; Frieman and Cormack, 2004; Halme *et al.*, 2004; Iraqui *et al.*, 2005); in addition, internal tandem repeats within genes coding for proteins with adhesive properties enable recombination events (Verstrepen *et al.*, 2004; Verstrepen *et al.*, 2005) and the formation of novel adhesins, thus providing fungi with an inexhaustible pool of adhesion possibilities.

2.2.1 Structure of adhesins

Yeast adhesins are composed of several domains with discrete functions. Their localisation on the outer surface determines their architecture and the following order of domains (Lipke and Kurjan, 1992; Shen *et al.*, 2001; Wojciechowicz *et al.*, 1993; Zhao *et al.*, 2001): N-terminal secretion signals, ligand binding domains, optional central Thr-rich glycosylated domains, N- and O-glycosylated stalks and C-terminal regions with glycosylphosphatidylinositol (GPI) anchors (see Figure 2.6).

The N-terminal secretion signals comprise 20-30 amino acids and are cleaved by a signal protease (Cappellaro *et al.*, 1994). The ligand binding domains exhibit properties similar to globular immunoglobulin-like structures (Terrance *et al.*, 1987), as their circular dichroism (CD) spectra are typical of β-sheet-rich folds. CD spectra of different adhesin domains also imply the presence of α-helices (Shen *et al.*, 2001).

The central tandemly repeated Thr-rich regions play a role in determining flocculation level. When the number of the repeats was manipulated, a linear relationship was observed between repeat number and flocculation, as well as strength of adhesion to polystyrene (Verstrepen *et al.*, 2005).

Stalks are rich in Ser/Thr content and usually exceed the length of 300 amino acid residues. Not much is known about the extent of glycosylation; however, the regions are predicted to form an expanded conformation (Gatti *et al.*, 1994; Jentoft, 1990), which hypothesis is supported by the stalk length visible in electron microghraph (Cappellaro *et al.*, 1994). Such length would allow for the ligand binding region to be sufficiently distant from the wall surface to enable its active functioning (Lipke and Kurjan, 1992). Indeed, deletion of some amino acids from this region results in inactive adhesins (Frieman and Cormack, 2003). Furthermore, two features of these regions have been described, yet not fully understood. First, substantial clusters of hydrophobic residues are present within the sequence. Second, the C-terminal areas of the Ser/Thr-regions are often rich in Cys residues. These form a disulphide network near the wall surface, presumably limiting the wall permeability by these means and also linking the adhesin to other GPI-anchored proteins (Huang *et al.*, 2003; Klis, 1994; Klis *et al.*, 2006).

GPI-linked proteins belong to two classes. While members of the first class are primarily membrane proteins and usually remain embedded within the membrane, the adhesins of the second class lose their association with the membrane and rather become cross-linked to other components of the wall (see Figure 2.7). Subsequent transglycosylation of truncated GPI glycans to β-1,6-glucans takes place (Klis, 1994; Kollar *et al.*, 1997; Lipke and Ovalle, 1998). The GPI moiety either remains membrane-attached, or is directed to the wall as well. Fate of this remaining part has not yet been characterised to a satisfactory degree; however, the sequence immediately preceding the GPI addition signal does influence its consecutive localisation to the membrane or the wall.

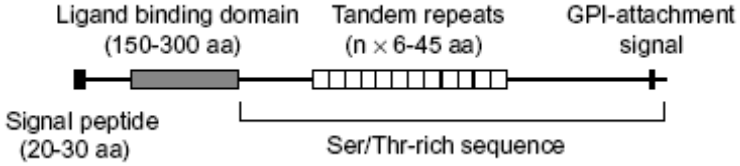

Figure 2.6 – A schematic modular organisation of fungal adhesins. The picture was taken from the paper of Linder and Gustafsson (2008).

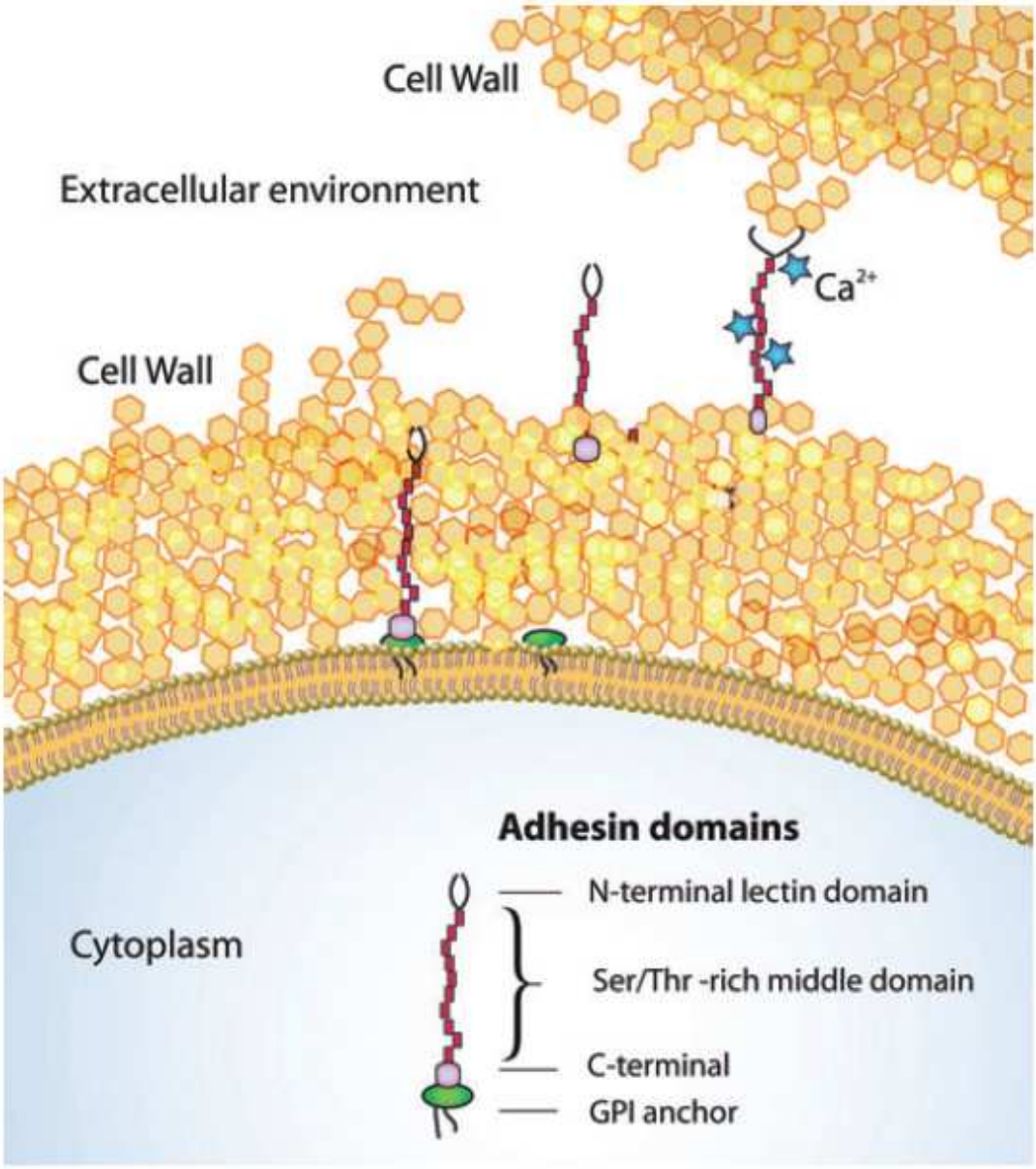

Figure 2.7 – Secretion and cell-surface anchoring of fungal adhesins. During transport through the secretory pathway, adhesins undergo extensive posttranslational modifications. In the endoplasmic reticulum the N-terminal signal peptide is removed and a C-terminal signal peptide is replaced by a GPI anchor; in addition, N-glycosylation and O-glycosylation are initiated. Further processing of the GPI anchor and the carbohydrate side-chains takes place in the Golgi apparatus (Bony *et al.*, 1997; De Groot *et al.*, 2003; Frieman and Cormack, 2003; Tiede *et al.*, 1999; Udenfriend and Kodukula, 1995). It is believed that the short O-linked oligosaccharide side-chains enable the adhesins to obtain a long, semi-rigid rod-like structure that is stabilized by Ca^{2+} ions (Jentoft, 1990). Upon arrival to the plasma membrane, the GPI anchor is cleaved off or the adhesin remains attached to the membrane (Frieman and Cormack, 2003; Frieman and Cormack, 2004). The picture was taken from (Verstrepen and Klis, 2006).

2.2.2 Mechanisms of adhesion

Adhesion can be divided into two main groups: lectin-like adhesion and sugar-insensitive adhesion. As the name suggests, the former type depends on the lectin-like binding of an adhesin to sugar residues on the surface of other cells. Adhesins of this group possess a lectin-like carbohydrate binding domain in their N-terminus. Addition of certain sugars competitively inhibits adhesion, thus providing an easy method to determine specificity of the adhesins. Members of this group include *Saccharomyces cerevisiae FLO* gene products, except for Flo11 (Guo *et al.*, 2000; Stratford, 1992). While the budding yeast adhesion was found to be mainly mannose-dependent (Kobayashi *et al.*, 1998; Miki *et al.*, 1982), the adhesive properties of its distant cousin, *Schizosaccharomyces pombe*, were found to be mediated predominantly by galactosyl residues (Tanaka *et al.*, 1999). The budding yeast lectin-like adhesion may be further divided into two subgroups, namely Flo1 and NewFlo. While the former only binds mannose sugars, the latter manifests ability to also bind different sugars, such as glucose or maltose apart from mannose (Sato *et al.*, 2002). Sugar-independent adhesion is mediated by adhesins either binding peptides, or inducing an increase in hydrophobicity of the cell surface (Kang and Choi, 2005). This group is represented by Flo11 adhesin of *Saccharomyces cerevisiae*, which confers adhesion to abiotic surfaces (Guo *et al.*, 2000), or Als proteins of *Candida albicans*, which grant this pathogen the capability of binding to host cells (Klotz *et al.*, 2004).

2.2.3 Regulatory pathways of adhesion

The adhesion genes are activated by diverse environmental triggers such as nutrient starvation (Sampermans *et al.*, 2005). The pathways regulating adhesion were best characterised for the *Saccharomyces cerevisiae FLO11* gene. The other *FLO* genes and also adhesins of pathogenic fungi are expected to be controlled by similar, although not identical signalling pathways (Lengeler *et al.*, 2000; Liu, 2001; Maidan *et al.*, 2005).

At least three well-known signalling cascades (see Figure 2.8) regulate the expression of *FLO11*: the Ras-cAMP pathway, the MAP kinase (MAPK)-dependent filamentous growth pathway and the main glucose repression pathway (Gagiano *et al.*, 2002; Madhani and Fink, 1997; Rupp *et al.*, 1999). A fourth pathway, the so-

called ‘Target of Rapamycin’ (TOR) pathway, has recently also been implicated in *FLO11* regulation (not depicted). This pathway is believed to respond to nitrogen starvation (Cutler *et al.*, 2001). A fifth (partial) pathway (not covered by the picture) involves the transcription factors Sok2, Phd1 and Ash1, which seem to function in an epistatic pathway; however, the details are not yet understood (Gimeno and Fink, 1994; Pan and Heitman, 2000; Ward *et al.*, 1995). In addition, a plethora of other genes have been shown to affect yeast adhesion in large-scale genetic screens (Verstrepen and Klis, 2006). Some of these genes may not be directly related to adhesion, but merely influence adhesion in an indirect way.

Rather little is known about the upstream sensors of the various signalling cascades. It is obvious that they are triggered by adhesion/flocculation activating conditions, such as nutrient limitation, stress inducing environment, or the proximity of a suitable infection site in case of pathogenic fungi. Even when the sensors actually are already identified, the picture is not straightforward, of which glucose serves as a good example: *FLO11* expression is repressed by the presence of glucose in the medium (the main glucose repression pathway). However, glucose is required for the Ras-cAMP/PKA pathway activation. Furthermore, the small G-protein Ras activates both the Ras/cAMP/PKA and MAPK pathways. Another component common for various signalling cascades is Mss11, apparently acting as a central regulator which integrates inputs of all three depicted pathways (van Dyk *et al.*, 2005). Hence it is clear that much remains to be investigated concerning the signalling cascades, their upstream sensors and conceivable cross-talk between them.

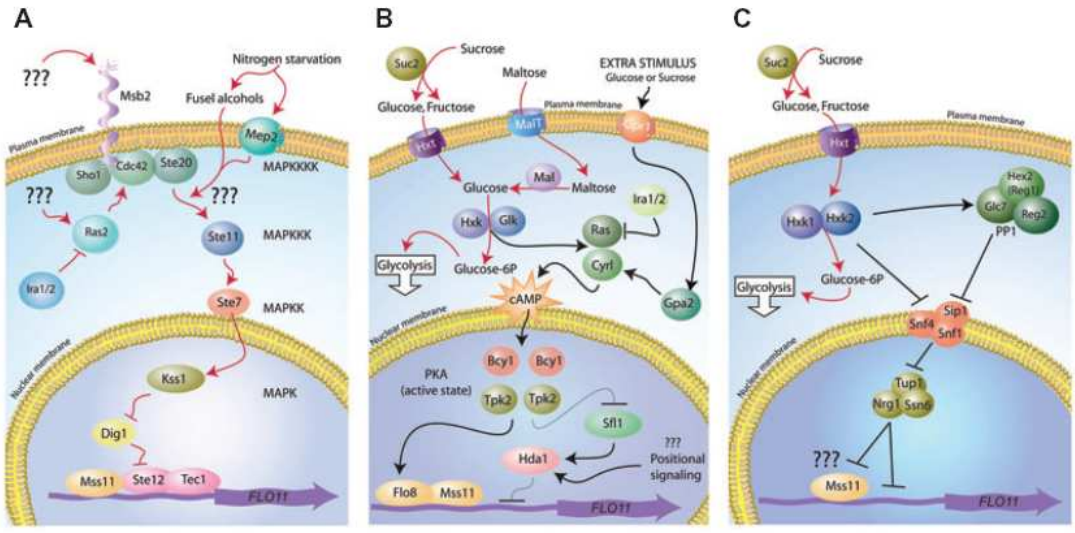

Figure 2.8 – The three main pathways regulating the expression of *FLO11*, see text for details. The picture was taken from (Verstrepen and Klis, 2006).

Very little is known about adhesins in the fission yeast. A number of *Schizosaccharomyces pombe* mutants that manifest flocculent phenotypes have been reported (Kim *et al.*, 2001; Samuelsen *et al.*, 2003; Tang *et al.*, 2003; Watson and Davey, 1998) but the only adhesins described in the fission yeast so far are the mating type-specific agglutinins Mam3 and Map4 (Mata and Bahler, 2006; Sharifmoghadam *et al.*, 2006).

The genomes of *Schizosaccharomyces pombe* and *Schizosaccharomyces japonicus* were screened using a molecular phylogenetic approach (Linder and Gustafsson, 2008). All of the putative fission yeast adhesins contained probable signal peptides at their N-termini but unlike previously characterised fungal adhesins, none of the adhesive proteins possessed detectable GPI anchor attachment signals (De Groot *et al.*, 2003; Eisenhaber *et al.*, 2004). The adhesins displayed a variety of conserved domains at their C-termini (see Figure 2.9). One of the identified regions is the DIPSY domain and with the data currently available it appears to be specific to the genus *Schizosaccharomyces* (Linder and Gustafsson, 2008). Another domain identified is also found in the *Saccharomyces cerevisiae* Flo11 protein and some other related species of Saccharomycotina, and thus was named Flo11 domain. From all the analysed adhesins containing the Flo11 domain the fission yeast SPBC1289.15 is the only one to have this domain situated at the C-terminus (Linder and Gustafsson, 2008). An uncharacterised domain with a conserved motif G(M/L)(E/A/N/Q)YA, hence named GLEYA, was identified. This domain was found to be related to the lectin-like ligand binding domain of the *Saccharomyces cerevisiae* Flo proteins (Linder and Gustafsson, 2008). Given that the fission yeast adhesins do not contain detectable GPI membrane anchor signals a novel cell wall attachment mechanism may be employed which yet remains to be elucidated.

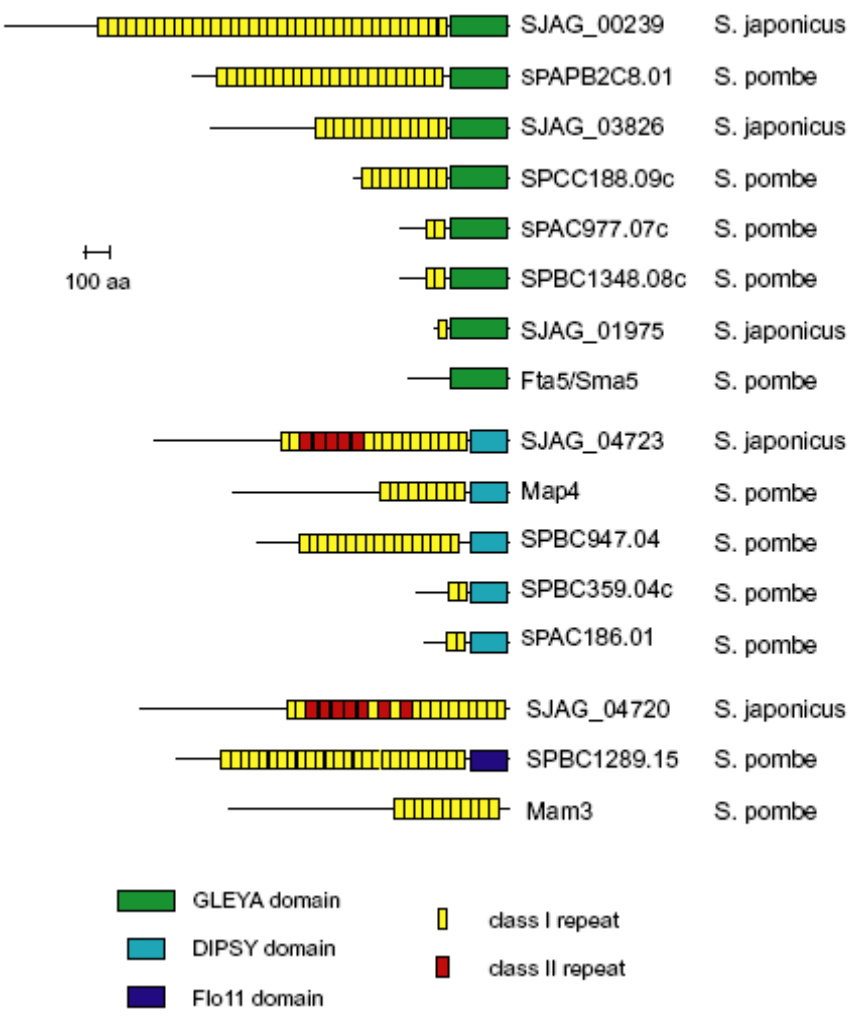

Figure 2.9 – Modular structure of adhesins in *Schizosaccharomyces pombe* and *Schizosaccharomyces japonicus.* The C-terminal domains identified are shown: GLEYA, DIPSY, and Flo11 in green, turquoise, and navy blue, respectively. Class I and class II repeats indicate a shorter and a longer repeat structure, respectively. The picture was taken from the paper of Linder and Gustafsson (2008).

2.2.4 Properties of adhesin genes

The genes coding for adhesive proteins are often under epigenetic control (Halme *et al.*, 2004). In a homogenous population of *Saccharomyces cerevisiae*, some cells do transcribe *FLO11*, while in other cells the gene remains silent. The expression state is usually inherited but reversible and cells can switch between the states. It is unknown whether mature cells are also capable of state switching or not. The epigenetic regulation of *FLO11* seems to be dependent on its subtelomeric localisation in the genome, as well as on the specific promoter of the gene, which partially relies on Ras/cAMP target proteins (see Figure 2.8). Similar regulation has been reported for other genes and organisms (De Las Penas *et al.*, 2003; Halme *et al.*, 2004), where the

chromatin remodelling complex Rap1/Sir3/Sir4 is required (Iraqui *et al.*, 2005,). In addition to these mechanisms, another activating way of silent adhesin genes was described (Halme *et al.*, 2004). The *IRA1* and *IRA2* genes contain an exceptionally high rate of nonsense mutations (10^{-3}). Their inactivation results in excessive activation of the Ras/CAMP/PKA pathway leading to de-silencing of *FLO10* gene. The unusually high incidence of *IRA* genes inactivation suggests that these mutations represent another mechanism of generating variability in the expression pattern of adhesins.

Epigenetic regulation is not exclusively an incidental switching mechanism. Chromatin remodelling is used to induce expression of the *Candida glabrata EPA6* gene in the host urinary tract (Domerque *et al.,* 2005). The de-silencing is probably caused by a decrease in NAD^+ concentration in the environment which affects the activity of the NAD^+-dependent histone deacetylase Sir2. On account of the higher levels of NAD^+ precursor nicotinic acid in blood during the bloodstream infection, *EPA6* activation does not occur in cells earlier than they enter the urinary tract.

Epigenetic regulation of adhesins serves multiple purposes. Silencing of adhesion in a subpopulation of cells provides a balance between adhering, colonising and non-adhering cells which can disseminate and colonise new sites. Epigenetic switching helps to anticipate new conditions in changing environment (Kussel and Leibler, 2005). Moreover, by only expressing a subset of adhesins, cells switch between appropriate adhesion phenotypes, allowing them to adhere to specific surfaces only.

The vast variability of adhesin genes has been reported in evolutionary studies where these genes were identified as one of the fastest expanding group of paralogs in the genomes of *Saccharomyces cerevisiae* and *Kluveromyces waltii* (Kellis *et al.*, 2004). Such variability results in a remarkable phenotypic variation in adhesion phenotypes between different but closely related strains and species (Verstrepen *et al.*, 2003). The highly repetitive DNA sequences in the middle part of the adhesin genes are the underbase of novel adhesins created (Verstrepen *et al.*, 2004; Verstrepen *et al.*, 2005). The repetitive nature and high sequence similarity trigger frequent slippage and/or recombination events during DNA replication which causes removal or addition of units, thus contraction or expansion of the adhesin gene, respectively. While shorter adhesins usually result in decreased adhesion, possibly because the N-terminal domain is not sufficiently exposed, longer adhesins generally confer greater adherence (Frieman *et al.*, 2002; Verstrepen *et al.*, 2005).

Similar to epigenetic regulation this mechanism also bestows fungal organisms to generate variability within a population and attune the adhesion properties. Furthermore, recombination between different adhesin genes may produce chimeric adhesins with diverse regulation and adhesive characteristics, thus allowing adherence to novel substrates. In pathogens such as *Candida albicans* or *Candida glabrata,* frequent recombination events of cell-surface genes combined with the variable expression of adhesins provide for a continuously changing surface which confers them the advantage of always being one step ahead of the adaptive immune system of their host.

3 *MATERIALS AND METHODS*

3.1 Microorganisms and cultivations

3.1.1 *Schizosaccharomyces pombe*

3.1.1.1 Cultivation, transformation and protein expression

Fission yeast strains (see Table 3.1) were cultured in the standard rich YES (0.5% yeast extract, 3% glucose, auxotrophic supplements as needed) and minimum MB (Formedium) media. Solid media were prepared from the liquid media by adding 2-3% agar. The G418 (100 µg/ml, Sigma) and/or ClonNAT (90 µg/ml, Werner Bioagents) antibiotics were added to YES for selection purposes where required. The standard cultivation temperature was 30°C.

For long-term storage cells were kept in 60% glycerol at -80°C, working batch of cells was kept at 10°C for up to 6 months. Freshly grown cells were prepared prior to each experiment. In some experiments, 5 µg/ml phloxin B, a red dye staining preferentially dead cells, was added to the media. Fission yeast diploid cultures contain a higher proportion of dead cells and therefore stain darker with phloxin B than haploids (Forsburg, 2003).

Where required, tenfold serial dilutions (10^5-10^1 cells) were prepared of washed cells from exponentially growing liquid cultures and spotted on the desired solid media in technical duplicates. Unless stated otherwise the spots were cultivated at 30°C for 5-7 days. Every sensitivity/resistance phenotype was at least once repeated in an independent biological replicate, so as to be confirmed credible.

Transformations were carried out using the lithium acetate method modifications as described in (Bahler *et al.*, 1998; Morita and Takegawa, 2004; Van Driessche *et al.*, 2005).

For inducible tagged protein expression the thiamine-repressible pREP-based vector series were used (Craven *et al.*, 1998) and the standard cultivation protocol was observed (Basi *et al.*, 1993).

3.1.1.2 Adhesion and flocculation assays

Cells were spotted or patched on YES or $MB_{-ura-thiamin}$ plates and grown at 30°C for various times. The adhesion assay based on a protocol described in (Guldal and Broach, 2006) consisted of washing the plates evenly with a stream of water for 1 min. The spot cell mass remaining attached to the plate was then documented by photography or microphotography using an Olympus CK2 light microscope with an Olympus SP-350 digital camera attached to it.

For flocculation assays, cells were grown in the appropriate YES or MB liquid media, either to the logarithmic or stationary phase, as required. Aggregation was monitored visually and the cell suspension was then transferred to a Petri dish for photography. The sugar-competition assays were performed as described in (Tanaka *et al.*, 1999). Cells from liquid culture were harvested, washed in 10 mM EDTA, and then in deionised water. Flocculation was initiated by the addition of 10 mM $CaCl_2$ in the presence or absence of 100 mM sugars. Cultures were transferred to a Petri dish for imaging.

Table 3.1 – *Schizosaccharomyces pombe* strains used.

Name	Genotype	Source
PN558	*h^+ leu1-32 ura4-D18 ade6-M210*	(Decottignies *et al.*, 2003)
PN559	*h^- leu1-32 ura4-D18 ade6-M216*	(Decottignies *et al.*, 2003)
CBF11-KO	*h^- leu1-32 ura4-D18 ade6-M216 Δcbf11::kan^r*	(Decottignies *et al.*, 2003)
MP01	*h^+ leu1-32 ura4-D18 ade6-M210 Δcbf12::pCloneNat1*	(Prevorovsky *et al.*, 2008)
MP03	*h^- leu1-32 ura4-D18 ade6-M216 Δcbf12::pCloneNat1*	(Prevorovsky *et al.*, 2008)
MP05	*h^+ leu1-32 ura4-D18 ade6-M216 Δcbf11::kan^r*	(Prevorovsky *et al.*, 2008)
MP07	*h^+ leu1-32 ura4-D18 ade6-M210 Δcbf11::kan^r Δcbf12::pCloneNat1*	(Prevorovsky *et al.*, 2008)
MP09	*h^- leu1-32 ura4-D18 ade6-M210 Δcbf11::kan^r Δcbf12::pCloneNat1$^-$*	(Prevorovsky *et al.*, 2008)
FY254	*h^- leu1-32 ura4-D18 ade6-M210 can1-1*	(Stolz, 2003)
Δvht1	*h^- leu1-32 ura4-D18 ade6-M210 can1-1Δvht1*	(Stolz, 2003)

3.2 Protein techniques

3.2.1 Protein electrophoresis

Proteins were separated by SDS-PAGE using the Mini-Protean 3 apparatus (Bio-Rad) and the standard Tris-glycine buffer system. 7.5% non-gradient gels were used as required. Proteins were stained with Coomassie Brilliant Blue G-250 (Bio-Rad) according to the manufacturer's instructions.

3.2.2 Western blotting and immunodetection

Proteins were transferred to a nitrocellulose membrane using the Mini Trans-Blot Module (Bio-Rad) and membranes were blocked with 2-3% milk. Appropriate primary and secondary antibodies (see Table 3.2) were applied and blots were developed with the ECL Western Blotting Detection Reagents (Amersham) according to the instructions of the manufacturers.

Table 3.2 – Antibodies used.

Name / Specificity	**Dilution**	**Source (Cat. no.)**	**Note**
His•Tag antibody (mouse monoclonal)	1 : 2000	Novagen (70796)	Primary antibody
goat anti-mouse IgG-HRP	1:10000	Santa Cruz Biotechnology (sc-2031)	Secondary antibody

3.3 DNA and RNA techniques

3.3.1 DNA isolation

Large scale plasmid preparations were performed using the standard alkaline extraction method (Birnboim and Doly, 1979) with an additional purification step comprising of precipitating protein impurities with 5 M lithium chloride. Every plasmid isolation was followed by restriction analysis confirming the plasmid identity. Chromosomal DNA preparations were carried out as described in (Hoffman and Winston, 1987).

3.3.2 Electrophoretic analysis of DNA in agarose gel

PCR products were separated by horizontal electrophoresis in the standard 1x TAE buffer. 2% gels were used as required. 5 µl of sample with 1 µl loading dye were loaded into wells. Gene Ladder Mix (SM0331) was used as a marker. DNA was stained with ethidiumbromide (0.5 µl/ml) and photographed under ultraviolet light.

3.3.3 RNA isolation

For qRT-PCR analyses, total fission yeast RNA was extracted using the FastPrep instrument (Q-BIOgene) and the RNeasy Mini kit supplemented with the RNase-free DNase set (Qiagen). The purity and concentration of the isolated RNA were measured on NanoDrop ND-1000 Spectrophotometer device (Thermo Scientific).

3.3.4 PCR and quantitative RT-PCR

3.3.4.1 PCR

The enzymes (see Table 3.3) were used according to the manufacturers' specifications; the primers (see Table 3.4) were used in 0.3 µM final concentration. Reactions were run on the Peltier PTC-200 gradient thermal cycler (MJ Research). Typically, the $MgCl_2$ concentration of 1.5 mM was used.

3.3.4.2 Quantitative real-time PCR

2 µg of total RNA extracted from each biological sample were reverse-transcribed with the RevertAid First Strand cDNA Synthesis Kit (Fermentas) and an oligo(dT) primer (total reaction volume 20 µl), 1 µl of cDNA was then used for amplification. Approximately 200 bp of the 3'-regions of *fip1*$^+$ (js01, js02), *frp1*$^+$ (js03, js04), *vht1*$^+$ (js05, js06), *str1*$^+$ (js07, js08), *str3*$^+$ (js09, js10), SPBC947.05c (js11, js12), SPAC1F8.02c (js13, js14), SPAC977.05c (js15, js16), SPCC1795.13 (js17, js18), SPBC359.04c (js19, js20), SPBC1348.02 (js21, js22) and *act1*$^+$ (mp37, mp38; normalisation control) were amplified in separate tubes using the primers indicated (see Table 3.4). The efficiency and linear range of the qRT-PCR were tested as described (Livak and Schmittgen, 2001). The qRT-PCR analysis was performed using the iQ SYBR Green Supermix (Bio-Rad) in the iQ^{TM}5 Multicolor Real-Time

PCR Detection System (Bio-Rad) with 0.3 μM each primer and the following program: 95°C for 3 min, 40× (95°C for 30 sec; 53°C for 30 sec; 72°C for 30 sec, 75°C for 15 sec). Three biological repeats were performed, the reactions were run in triplicates and data were analysed in the iQ^{TM}5 Optical System Software (Bio-Rad).

Table 3.3 – PCR and qRT-PCR systems used.

System	**Source**
Taq DNA polymerase	Fermentas
RevertAid First Strand cDNA Synthesis Kit	Fermentas
iQ SYBR Green Supermix	Bio-Rad

Table 3.4 – Oligonucleotide primers used.

Primer	**Sequence**	**Purpose**
js01	TTTATGTTCTTCGACGGGAG	*fip1*$^{+}$, qRT-PCR (fwd)
js02	ATGTGGTACAAGGAACGTCG	*fip1*$^{+}$, qRT-PCR (rev)
js03	AAGATCGACAGTGGAAGGTG	*frp1*$^{+}$, qRT-PCR (fwd)
js04	CCTGTCGAGGAAGTCTCTTC	*frp1*$^{+}$, qRT-PCR (rev)
js05	TCATCTCTTGCTCGTCTTCC	*vht1*$^{+}$, qRT-PCR (fwd)
js06	ATTTGGGATCTGTCGTTACG	*vht1*$^{+}$, qRT-PCR (rev)
js07	ATGATGGCATTTCTAGCGTC	*str1*$^{+}$, qRT-PCR (fwd)
js08	CACAGCCCTTGTTAGTACCG	*str1*$^{+}$, qRT-PCR (rev)
js09	TTGTGTGGTTTCTTTGTCCC	*str3*$^{+}$, qRT-PCR (fwd)
js10	TAAGAGAGTATCCCGTTGGC	*str3*$^{+}$, qRT-PCR (rev)
js11	TTTACGGAGTTTTTGATGCG	SPBC947.05c, qRT-PCR (fwd)
js12	ATAAACCATTTTACCGGCAG	SPBC947.05c, qRT-PCR (rev)
js13	AGGAATCAGAAGAATCAGCC	SPAC1F8.02c, qRT-PCR (fwd)
js14	TGGTGGTGATGGAAATAAGC	SPAC1F8.02c, qRT-PCR (rev)
js15	ACAATAACGCAGAGAATCCG	SPAC977.05c, qRT-PCR (fwd)
js16	TTTGAAAACATGCAATCCTC	SPAC977.05c, qRT-PCR (rev)
js17	GAGACAAACGTCAAATAGGC	SPCC1795.13, qRT-PCR (fwd)
js18	AGCACCTGAAAGCAGTACTG	SPCC1795.13, qRT-PCR (rev)
js19	CCTACATCATCCATACCACC	SPBC359.04c, qRT-PCR (fwd)
js20	TTAACTTGTGATTGCGTACG	SPBC359.04c, qRT-PCR (rev)
js21	GAATACACCCAAATTGCAGG	SPBC1348.02, qRT-PCR (fwd)
js22	GTGATTTACTGTGCATTGGG	SPBC1348.02, qRT-PCR (rev)
mp37	GTAAACGATACCAGGTCCGC	*act1*$^{+}$, qRT-PCR (fwd)
mp38	GGTACCACTATGTATCCCGG	*act1*$^{+}$, qRT-PCR (rev)

The sequences are given in the 5'-3' orientation. The primers were designed using GeneRunner 3.04 (Hastings Software) and synthesized by Agowa. fwd – forward primer, rev – reverse primer.

3.3.4.3 Analysis of qRT-PCR data

Raw data acquired were subjected to filtering. First, failed reactions were removed from following analysis. Each data set was examined visually in order to exclude amplification curves, whose continuance was not satisfactory (e.g. exhibited distortions in comparison to a smooth sigmoid curve). Similarly, melting curves were controlled.

Next, variability within the reaction triplicates was revised. If any standard deviation value exceeded the threshold of 0.300, the one reaction of the corresponding triplicate was excluded from further analysis whose C_T (threshold cycle) was considered most divergent from the remaining two. After this selection mathematical tools were applied (see Section 3.3.4.3.1 and 3.3.4.3.2).

Lastly, the three biological replicates were confronted and the final selection performed in order to remove extreme values in a systematic manner. Corresponding values of appropriate gene and strain acquired from the raw data analysis were compared and again, the one most different from the others was removed (see Section 3.3.4.3.3).

3.3.4.3.1 Relative quantification

Normalising to an endogenous reference (*act1*$^+$ in our experiment) provides a method of correcting results for differing amounts of input cDNA (Livak and Schmittgen, 2001). The operation involves subtraction of C_T values for target and reference genes and is described by the following equation:

$$\Delta C_T = C_{T,\,(\text{target gene})} - C_{T,\,(\text{endogenous reference})}$$

The amount of target relative to endogenous reference is then:

$$\text{amount of target} = 2^{-\Delta Ct}.$$

3.3.4.3.2 Comparison to control

This quantification describes the change in expression of the target gene relative to some reference group, e.g. an untreated control. Usually, the simplest design is to take the untreated control for the calibrator. For the untreated control sample, $\Delta\Delta C_T$ equals zero and 2^0 equals one, so that the fold change in gene expression relative to

the untreated control equals one, by definition. For the treated samples, evaluation of $2^{-\Delta\Delta Ct}$ indicates the fold change in gene expression normalised to and endogenous reference and relative to the untreated control. The equation describing $-\Delta\Delta C_T$ for a target is:

$-\Delta\Delta C_T = -(\Delta C_T,s - \Delta C_T,cb)$ s – sample, cb – calibrator.

Thus, the amount of target normalised to an endogenous reference and relative to a calibrator is given by:

amount of target = $2^{-\Delta\Delta Ct}$.

3.3.4.3.3 Comparison of biological replicates

To compare the three biological replicates, the corresponding results of $2^{-\Delta Ct}$ for gene and strain were confronted. The following formulas were used for each triplicate of values:

X = MEDIAN(A1:A3)/MIN(A1:A3)
Y = MAX(A1:A3)/MEDIAN(A1:A3)

where (A1:A3) stands for the respective triplicates. The successive logical condition was then applied, so as to remove the minimal extreme value, if the condition was fulfilled, or the maximal extreme value, if the condition was not fulfilled:

=IF(X>Y;MIN(A1:A3);MAX(A1:A3)

3.3.4.4 Quantitative real-time PCR workflow

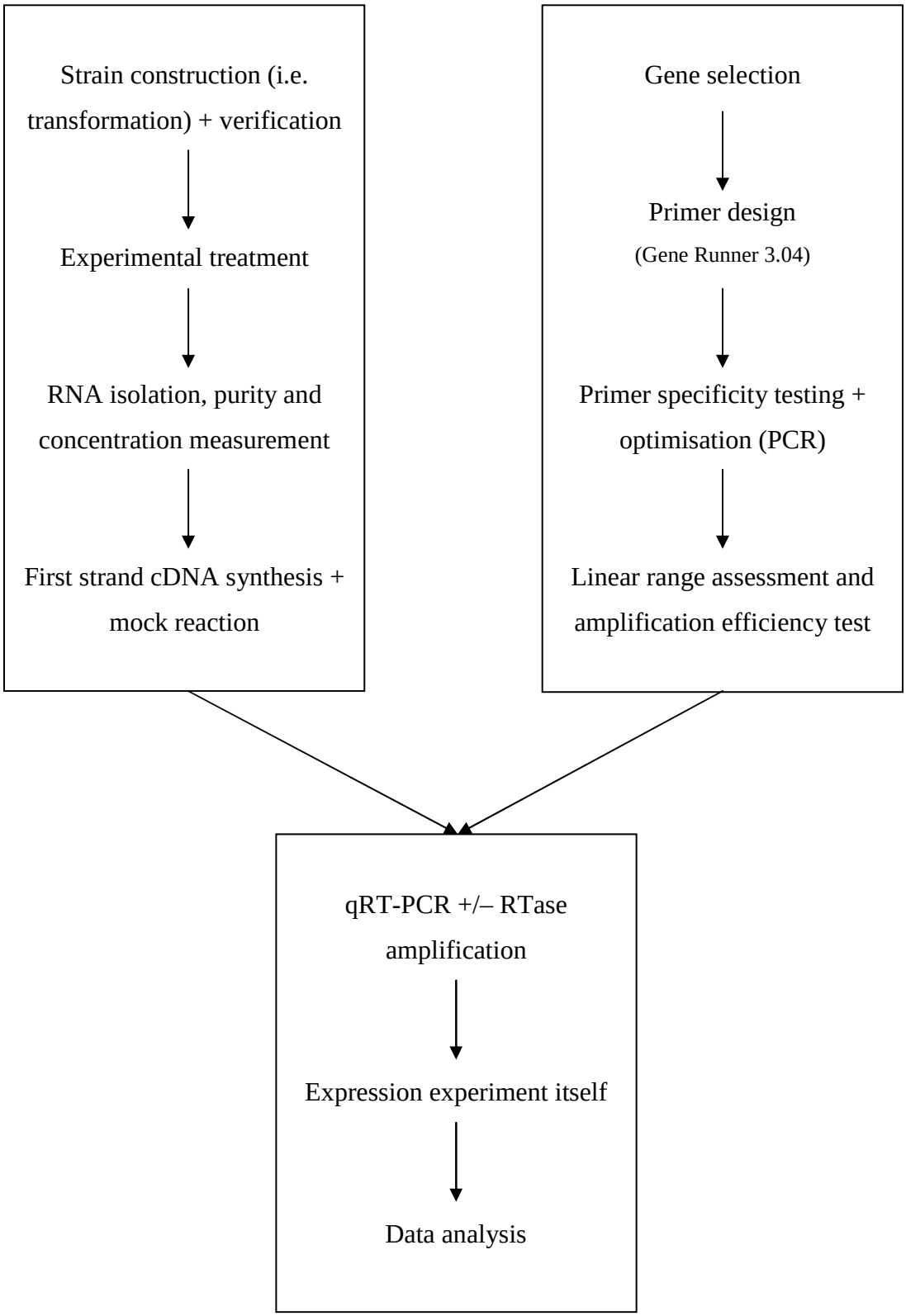

3.3.5 Plasmids

The following plasmids were used (see Figures 3.1-3.3):

Table 3.5 – Plasmids used in this study.

Name	Backbone	Size in bp (total/insert)	Description	Cloning method
	pREP42MHN	8396/---	control plasmid	
pMP32	pREP42MHN	11289 / 2893	MycHis-Cbf12 expression in *Schizosaccharomyces pombe*	*Nde*I / *Bgl*II into *Nde*I / *Bam*HI
pJR08	pREP42MHN	10246 / 1850	MycHis-Cbf11 expression in *Schizosaccharomyces pombe*	*Nde*I / *Bam*HI

The plasmid maps were modified using Clone Manager 4.

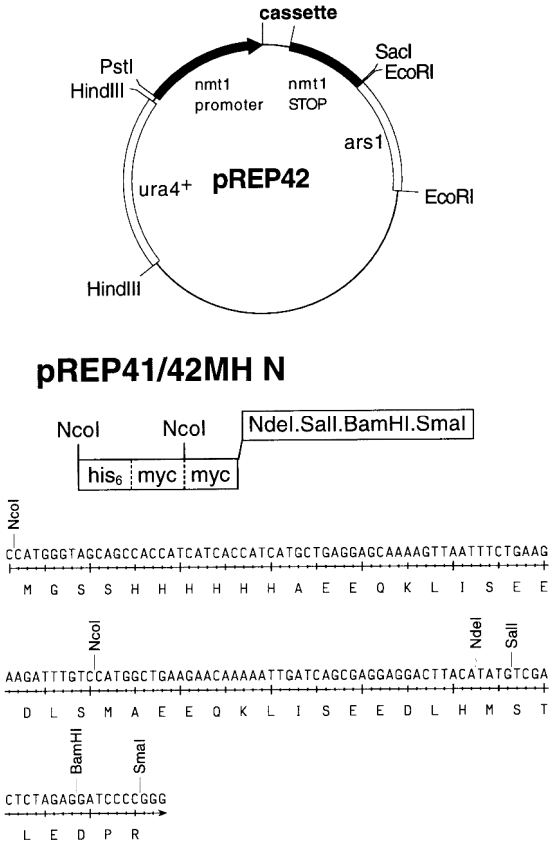

Figure 3.1 – Plasmid pREP42MHN used as empty vector.

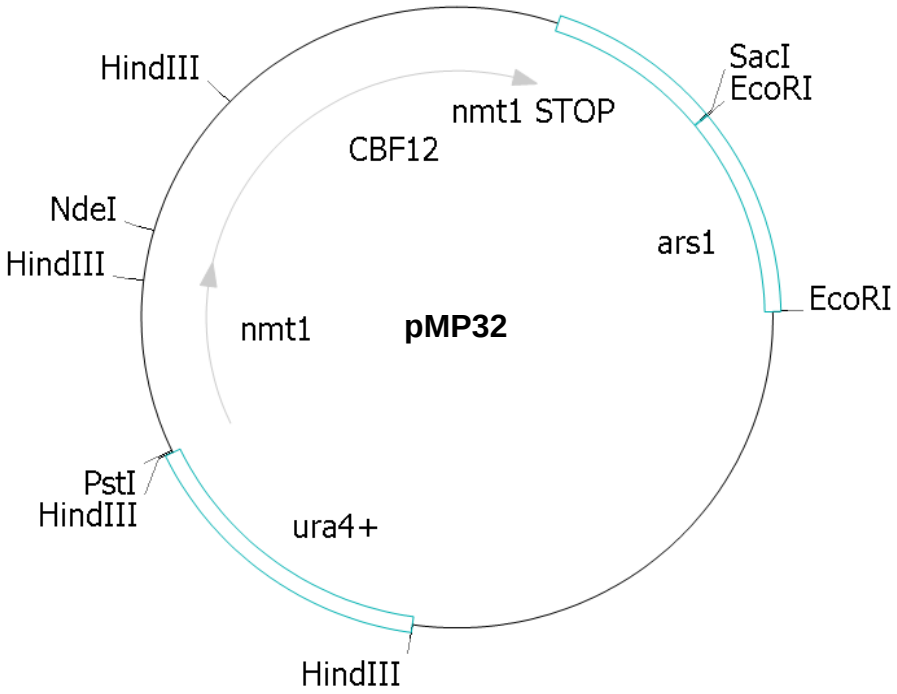

Figure 3.2 – Plasmid pMP32 used for overexpression of tagged Cbf12.

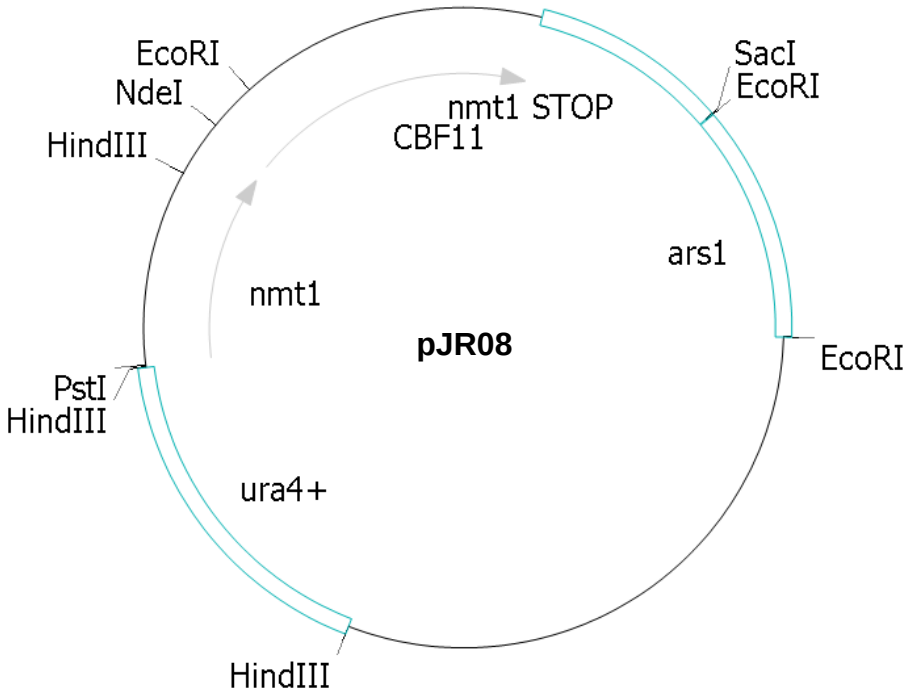

Figure 3.3 – Plasmid pJR08 used for overexpression of tagged Cbf11.

3.4 Microscopy and imaging

3.4.1 Fluorescence and bright field microscopy

Where required, nuclei were stained with DAPI (1 μg/ml). The mounting medium consisted of 23% glycerol, 9% mowiol, 27.3 mM PIPES, 11.3 mM HEPES, 4.5 mM EGTA, 0.45 mM $MgCl_2$, pH 8.3. DABCO was added as antifade (50 mg/ml) prior to mounting.

Confocal fluorescent images were acquired using a Leica TCS SP2 confocal microscope and the accompanying software. Epifluorescence images were taken with either an Olympus IX81 microscope and the cell^R 2.6 software (Olympus) or a Nikon Eclipse TE2000-S microscope and the NIS Elements imaging software (Nikon).

3.4.2 Colony imaging

High-magnification colony images were taken by a Hitachi HV-C20 camera connected to a Navitar Zoom 6000 optical system and the NIS Elements imaging software (Nikon). Agar plates under low magnification were photographed using a Kodak DC290 Zoom or a Panasonic DMC-FZ7 camera.

3.5 Bioinformatics and software

Table 3.6 – Databases and bioinformatics tools used.

Name	Description / URL	Source
NCBI databases	Protein and nucleotide sequence database http://www.ncbi.nlm.nih.gov/sites/gquery	
GeneDB	*Schizosaccharomyces pombe* genome database, annotations and bioinformatics tools http://www.genedb.org/genedb/pombe/	(Hertz-Fowler *et al.*, 2004; Wood *et al.*, 2002; Aslett and Wood, 2006)

4 *RESULTS*

4.1 Phenotypes of the Δ*cbf11* and Δ*cbf12* single and double deletion strains

4.1.1 Growth phenotypes, sensitivity and resistance tests

One of the classical methods to determine functions of a gene is creation of a mutant strain bearing deletion of the gene, and its successive analysis. The deletion strains may exhibit behaviour different to that of the wild type strain, which, provided that there are no other genome alterations than the desired gene deletion, would point out the engagement of this gene in the affected processes.

A Δ*cbf11* strain had already been prepared (in a diploid strain) in a fission yeast genome-wide deletion project (Decottignies *et al.*, 2003). The strain was constructed using a standard targeted PCR-based gene deletion procedure (Bahler *et al.*, 1998) and the *cbf11*$^+$ open reading frame (ORF) was replaced with a kanamycin resistance cassette by homologous recombination. A haploid *h*$^-$ Δ*cbf11* strain CBF11 KO and the parental strains PN558 (*h*$^+$) and PN559 (*h*$^-$) were obtained from Dr. Anabelle Decottignies, Cancer Research UK. The deletion was crossed into cells of the *h*$^+$ mating type, MP05 (Prevorovsky *et al.*, 2008), in order to facilitate testing of possible functions specific for a mating type.

A Δ*cbf12* strain had also been prepared previously during a large-scale study of uncharacterized, meiotically upregulated genes (Gregan *et al.*, 2005). However, the deletion had been constructed in *h*^{90} cells capable of switching mating type, and therefore not suitable for our experiments. Thus, the targeting vector (Gregan *et al.*, 2005) was used to construct the heterothallic *h*$^+$ and *h*$^-$ Δ*cbf12* strains from PN558 and PN559, respectively (Prevorovsky *et al.*, 2008). By these means, the *cbf12*$^+$ ORF was replaced by a nourseothricin resistance cassette. To allow for investigating the possibility of crosstalk between the two CSL paralogs, double deletion heterothallic strains were constructed (Prevorovsky *et al.*, 2008).

We then subjected the respective deletion strains MP01, MP03 (*cbf12*$^+$ deletion), CBF11 KO, MP05 (*cbf11*$^+$ deletion), MP07, MP09 (*cbf12*$^+$ *cbf11*$^+$ deletions); and the wild type controls PN558 and PN559 (see Table 3.1) to standard growth and sensitivity/resistance tests as to identify the effects of the respective deletions to help

us understand the function of CSL genes in *Schizosaccharomyces pombe*. The stressors were selected on the basis of the paper by Bimbó *et al.* (2005), in order to obtain results possibly comparable with data previously published and to test a wide variety of different conditions activating diverse response pathways. Unfortunately, no comparison with the data of Bimbó *et al.* (2005) could be made.

When liquid cultures for spot tests were prepared, growth impairment of strains with *cbf11*$^+$ deletion was observed. In order to study this defect more closely, growth curves for shaken cultures in rich media at 30°C were measured (see Figure 4.1). While the *cbf12*$^+$ deletion strains showed no difference from the WT control, Δ*cbf11* strains exerted protracted growth. Δ*cbf11* Δ*cbf12* cultures manifested even greater growth impairment than the single *cbf11*$^+$ deletion strains did, which is indicative of possible crosstalk between the two paralogs.

All mutant strains exhibited viability comparable to WT controls when serial dilutions were spotted on minimal medium plates or rich medium plates and also when exposed to heat, osmotic and salt stress, or in the presence of various substances affecting DNA replication, calcium signalling, translation, or damaging the plasma membrane, cell wall and cytoskeleton, and causing oxidative stress induced by H_2O_2 (data not shown; see Table 4.1 for the list of treatments).

However, growth of the strains lacking *cbf11*$^+$ was found to be strongly impaired on rich media at 19°C. Apart from this phenotype, the above stated treatments gave no significant results which prompted us to perform further tests with the treatment selection based on microarray results of Prevorovsky (unpublished data) and their similarity to the microarray profiles of Mediator mutants. Thus, biotin excess/starvation (data not shown), iron excess/starvation, formamide, caffeine and cadmium were chosen for the additional analysis.

Indeed, when spotted on solid media containing 2.3% formamide, 0.1 mM cadmium or 11 mM caffeine, the Δ*cbf11* strains displayed sensitivity to the respective agents (see Figures 4.2-4.6). On the contrary, the growth on solid media with 4 mM $FeCl_2$ added showed resistance of the *cbf11*$^+$-lacking strains to such oxidative stress/heavy metal (see Figure 4.7).

Table 4.1 – Sensitivity/resistance tests used.

Treatment/Medium	Dosing	Description
MB	N/A	minimal defined medium
YES	N/A	complete rich medium
19˚C	N/A	cold stress
36˚C	N/A	heat stress
EGTA	5-40 mM	disruption of calcium signalling
hydroxyurea	7.5-11.25 mM	inhibition of DNA replication
KCl	0.4-1.2 M	osmotic/salt stress
sorbitol	1.2-2.0 M	osmotic stress
SDS	0.003-0.01%	disruption of membranes
calcofluor	100-800 mg/ml	cell wall damage
cycloheximide	10-40 mg/ml	inhibition of proteosynthesis
latrunculin A	0.25-1.0 mM	disruption of actin cytoskeleton
carbendazim	10-25 mg/ml	inhibition of microtubule polymerisation
biotin	0-200 µg/l	excess of vitamin H
avidin	1.1-5.5 mg/l	vitamin H starvation
H_2O_2	1-10 mM	oxidative stress
$CdCl_2$	0.05-0.95 mM	oxidative stress/heavy metal
$FeCl_2$	1-10 mM	oxidative stress/heavy metal
ferrozine	0.3-2.0 mM	iron starvation
caffeine	10-13 mM	interference with purine metabolism
formamide	1.5-3.0 mM	disruption of proteins and RNA molecules

Unless stated otherwise, YES medium was used as a basis.

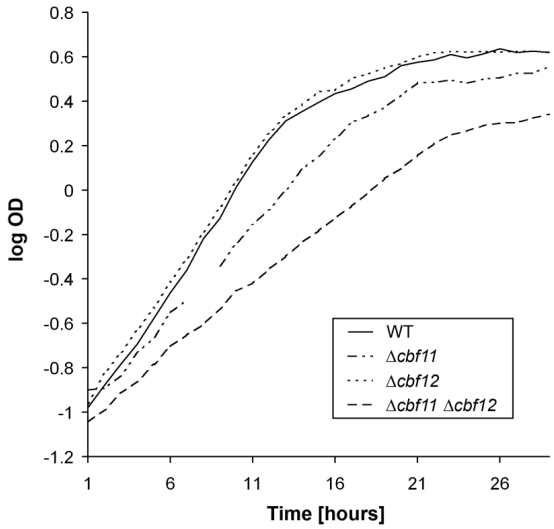

Figure 4.1 – Deletion of *cbf11*$^+$ causes slow growth. The cells were cultured at 30°C in YES and optical density was measured every hour. There is no difference between the Δ*cbf12* strain and WT. On the contrary, deletion of *cbf11*$^+$ results in growth protraction, which phenotype is accentuated by the simultaneous deletion of *cbf12*$^+$.

	10^5	10^4	10^3	10^2	10^1
Δcbf12					
Δcbf11					
Δcbf11 Δcbf12					
WT					

Figure 4.2 – Growth in optimal settings on rich media at 30°C shown for comparison. The table indicates the order of strains and numbers of cells spotted.

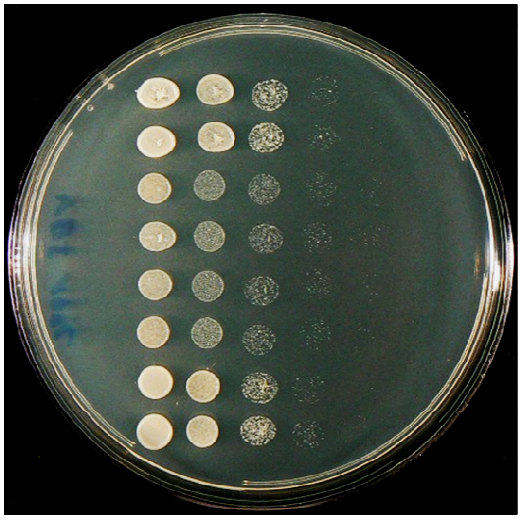

	10^5	10^4	10^3	10^2	10^1
Δcbf12					
Δcbf11					
Δcbf11 Δcbf12					
WT					

Figure 4.3 – Growth on rich media at 19°C. Strains lacking *cbf11*$^+$ display sensitivity to low temperature when compared with WT or Δ*cbf12* strains.

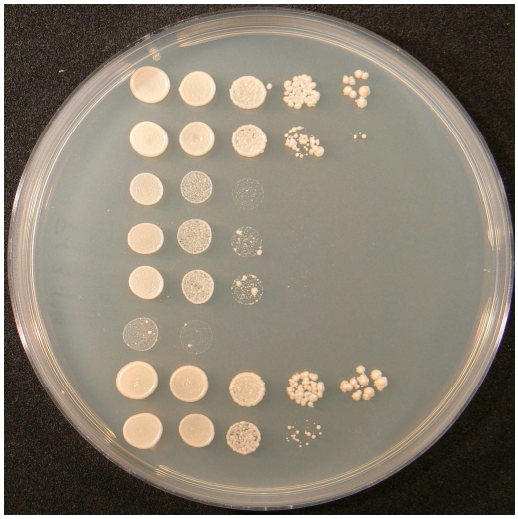

	10^5	10^4	10^3	10^2	10^1
Δcbf12					
Δcbf11					
Δcbf11 Δcbf12					
WT					

Figure 4.4 – Growth on media with 2.3% formamide added. Strains harbouring deletion of *cbf11*$^+$ exert impaired growth in comparison with WT controls or *cbf12*$^+$-lacking strains. For unknown reasons one of the strains bearing simultaneous deletions of *cbf11*$^+$ and *cbf12*$^+$ shows high sensitivity to formamide when compared with its partner.

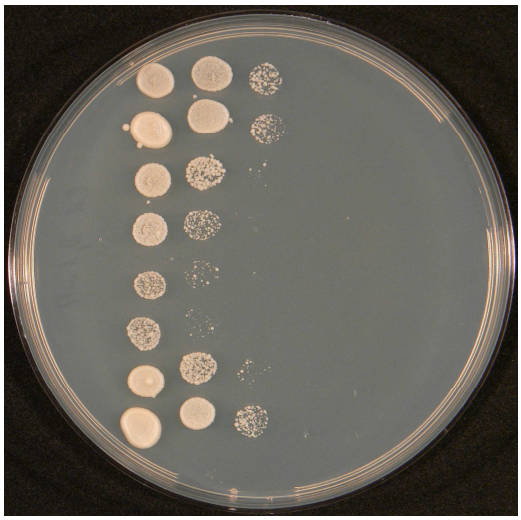

	10^5	10^4	10^3	10^2	10^1
Δcbf12					
Δcbf11					
Δcbf11 Δcbf12					
WT					

Figure 4.5 – Growth on media with 0.1 mM $CdCl_2$ added. Strains harbouring deletion of *cbf11*$^+$ exhibit impaired growth in comparison with WT controls or *cbf12*$^+$-lacking strains, which effect was found to be accentuated in case of simultaneous deletions of both CSL genes.

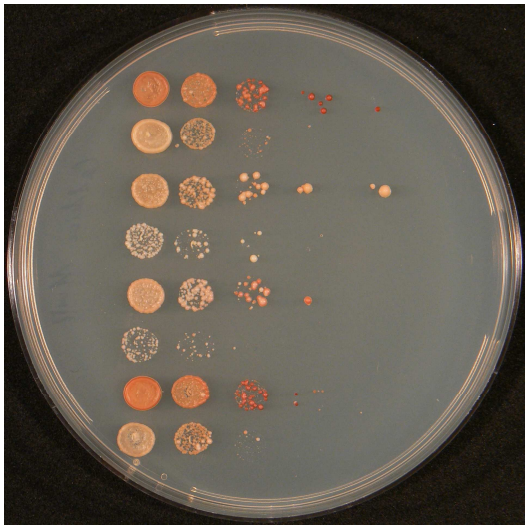

	10^5	10^4	10^3	10^2	10^1	
Δcbf12						h^+
						h^-
Δcbf11						h^+
						h^-
Δcbf11 Δcbf12						h^+
						h^-
WT						h^+
						h^-

Figure 4.6 – Growth on media with 11 mM caffeine added. Here, h^+ strains and h^- strains are not comparable, as the h^- cells manifest a more sensitive phenotype when compared with their h^+ partners. Taken separately, the h^+ Δ*cbf11* deletion strains show impaired growth in contrast to the matching h^+ WT or Δ*cbf12* cells (best visible in the second line from the left). Similarly, the h^- Δ*cbf11* cells exert analogous phenotype when confronted with their corresponding WT or *cbf12*$^+$-lacking counterparts (best visible in the second line from the left).

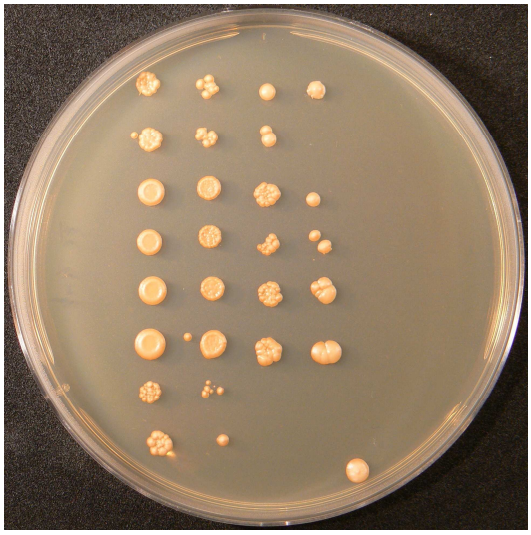

	10^5	10^4	10^3	10^2	10^1
Δcbf12					
Δcbf11					
Δcbf11 Δcbf12					
WT					

Figure 4.7 – Growth on media with 4 mM $FeCl_2$ added. Strains lacking *cbf12*$^+$ grow better than the WT controls. While the Δ*cbf11* strains display even stronger resistance, strains with combined deletions of both CSL genes exhibit the highest tolerance to the presence of $FeCl_2$ in comparison with the others.

Fission yeast strains harbouring deletions of *cbf11*$^+$ and *cbf12*$^+$, respectively, exert sensitivity to formamide, caffeine and cadmium, and resistance to excess of iron at the same time. Taken together, our results obtained from growth and sensitivity/resistance tests suggest a role for the respective CSL genes in response to disruption of proteins and RNA molecules, interference with the metabolism of purines and oxidative stress caused by different substances in *Schizosaccharomyces pombe* cells.

4.1.2 Colony morphology

While performing the spot tests series, we noticed macroscopically visible differences between the colonies of WT strains and Δ*cbf12* strains, and *cbf11*$^+$ deletion strains grown on the rich medium. That is, when illuminated from a specific angle, the surface of the spotted WT and Δ*cbf12* giant colonies appeared dim, which was in contrast to the Δ*cbf11* and Δ*cbf11* Δ*cbf12* giant colonies, the surface of which reflected much more light, displaying a 'shiny' phenotype (see Figure 4.8A). When the colonies were gently submerged in water, a thin floating layer of the 'shiny' material came off the colony surface (see Figure 4.8B). Thus, it is likely that the 'shiny' phenotype is caused by overproduction of some extracellular material containing hydrophobic and reflective compounds. Under higher magnification the surface of the 'shiny' spots appeared to be grooved, while, on the contrary, the surface of the dim giant colonies was smooth (see Figure 4.9A). Interestingly, the 'shiny' phenotype was never observed on minimal media.

Next, the morphology of monocolonies was studied. The monocolonies were left to grow for a long period of time (14 days). In order to visualize the physiological state of cells phloxin B (a dye preferentially staining dead cells) was added into the medium. The phenotypes displayed in these settings were consistent with the results acquired with giant colonies (see Figure 4.9A). The WT and Δ*cbf12* strains formed regular and evenly stained colonies, while the Δ*cbf11* and Δ*cbf11* Δ*cbf12* strains' colonies showed marked alterations. Their colonies were irregular in shape with sectors of cell populations staining darker than the surrounding areas (see Figure 4.9B). This phenotype will be dealt with more thoroughly in the next section.

A rescue experiment performed by another member of our team showed that the overexpression of *cbf11*$^+$ in a double deletion strain could suppress the phenotype of

altered colony morphology (Prevorovsky *et al.*, 2008). On the other hand, the overexpression of *cbf12*$^{+}$ in the same background resulted in a staining even darker than that of double deletion colonies transformed with an empty vector only, which indicates that the high dosage of *cbf12*$^{+}$ is toxic for the cells (Prevorovky *et al.*, 2008).

In summary, the deletion of *cbf11*$^{+}$ leads to various changes in the morphology of giant colonies and monocolonies of fission yeast cells, suggesting possible engagement of Cbf11 in the establishment of cell-cell contact. However, the Cbf11 involvement in these processes may not be straightforward – a plausible reason for the dissimilarity of the Δ*cbf11* colonies may be a changed morphology of the cells (see Section 4.1.3) or their different adhesive properties (see Section 4.1.4); moreover, both explanations may combine.

A

B

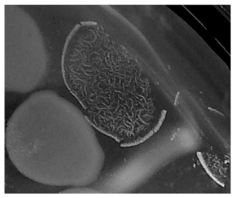

Figure 4.8 – 'Shiny' phenotype. Cells were spotted on a YES plate and incubated in standard settings. (A) The Δ*cbf11* and Δ*cbf11* Δ*cbf12* strains display a 'shiny' phenotype when illuminated in contrast to the dim colonies of WT and Δ*cbf12*. (B) A thin, floating layer comes off, when the colony is gently submerged in water.

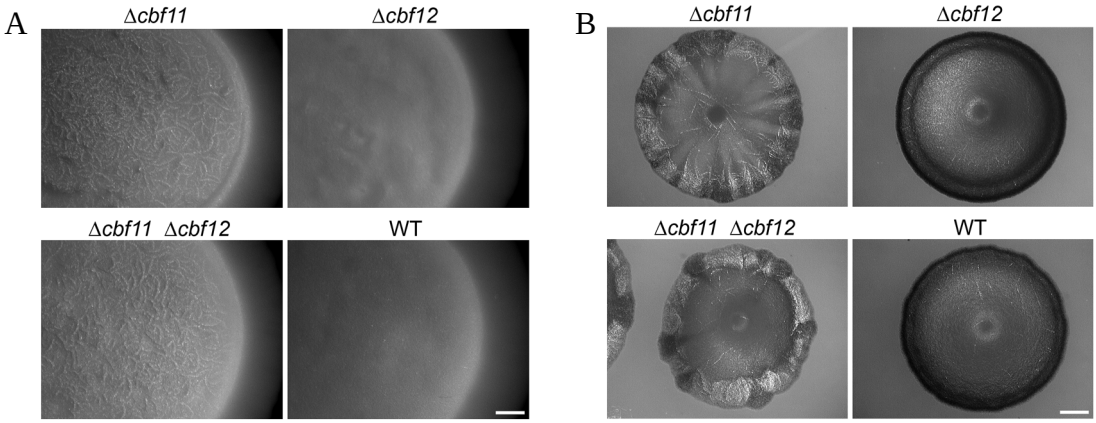

Figure 4.9 – Morphology of giant colonies and monocolonies. (A) Spots were cultivated in standard settings for 7 days. Surface of the WT and Δ*cbf12* dim giant colonies is smooth in contrast to the grooved surface of the Δ*cbf11* and Δ*cbf11* Δ*cbf12* 'shiny' giant colonies. The bars represent 1 mm. (B) Monocolonies were grown for 14 days on YES plates containing phloxin B. The colonies of the Δ*cbf11* and Δ*cbf11* Δ*cbf12* strains are irregular in shape and display sectoring. The Δ*cbf12* monocolonies appear normal, as those of WT strain do.

4.1.3 Cell morphology

When studying colony morphology of our respective deletion strains, we observed that Δ*cbf11* and Δ*cbf11* Δ*cbf12* strains' colonies displayed dark sectoring of phloxin B staining (see Figure 4.9B). In *Schizosaccharomyces pombe*, such dark staining is typical for diploid colonies (Forsburg, 2003), suggesting that the dark sectors might represent diploid clones arising in the mutant populations. The colonies were assayed by flow cytometry (FACS) as to determine the ploidy of these clones. Indeed, other members of our team obtained data confirming the presence of diploid subpopulations (Prevorovsky *et al.*, 2008). Since the light and dark sectors were also analysed separately, the dark sectors could unequivocally be determined as the diploid clones.

This incited us to analyse the CSL deletion strains microscopically. Importantly, all strains were heterothallic, either h^+ or h^-, unable to switch mating types, hence incapable of self-conjugation. We assayed both live and fixed cells from exponentially growing cultures. While there were practically no alterations present in the WT controls and only few in the Δ*cbf12* strains, the *cbf11*$^+$-lacking cells showed various defects (see Figure 4.10). The phenotypes could generally be described as consequences of cellular and nuclear division failed coordination, including

heterogeneity in cell size and shape, and frequent large cells with diploid-like nuclei that probably corresponded to the diploid fraction observed by FACS. Very large cells with giant, possibly polyploid nuclei were also seen, although seldom (see Figure 4.10E, right). We also noticed the so-called 'sep' phenotype (Grallert *et al.*, 1999), manifested by diverse septation defects subsuming multisepta in a single cell, aberrant septum structures and pseudohyphal growth. The highest incidence of the 'sep' phenotype was observed in the double deletion and the Δ*cbf11* strains (9.4% and 6.2%, respectively). Lastly, the deletion of *cbf11*$^+$ was found to be associated with the 'cut' (cell untimely torn) phenotype (Hirano *et al.*, 1986), again most frequent in the double deletion and Δ*cbf11* strains (22.8% and 13.0%, respectively). This phenotype is a result of the septum often forming prematurely, thus either cutting across the nucleus (if such cells separate, the cut nuclei remain attached to the former septum; see Figure 4.10D), or missing the nucleus and producing one anucleate and one possibly viable 'diploid' compartment, respectively. The 'cut' phenotype might thus be responsible for the diploidisation we observed.

Another member of our team also analysed the overexpressor strains microscopically. While the overexpression of *cbf11*$^+$ was well tolerated by the cells, the high dosage of c*bf12*$^+$ resulted in phenotypes equivalent to those observed in Δ*cbf11* cells. Interestingly, the 'cut' phenotype was almost never detected in the *cbf12*$^+$ overexpressor strain (Prevorovsky *et al.*, 2008).

Taken together, the lack of *cbf11*$^+$ or excess dose of *cbf12*$^+$ both result in diverse defects in cellular and nuclear division (Prevorovsky *et al.*, 2008), confirming the requirement for physiological levels of CSL proteins in these processes.

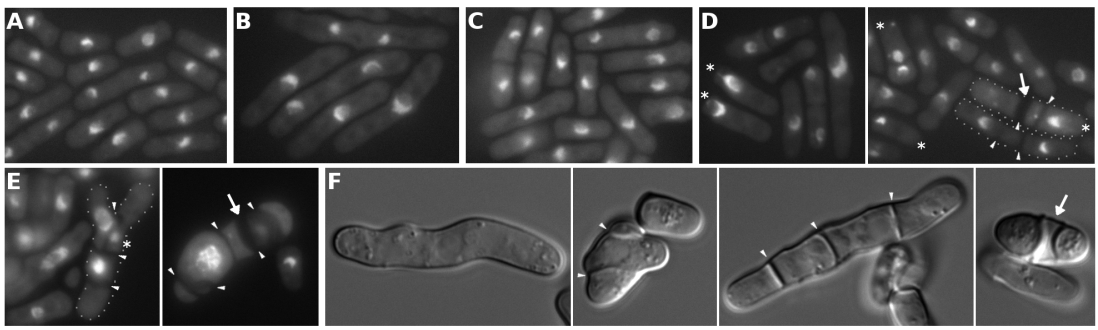

Figure 4.10 – Loss of *cbf11*$^+$ leads to multiple defects in cellular and nuclear division. Exponentially growing cells, either live (F) or fixed with ethanol and stained with DAPI (A-E), were observed under an epifluorescence/DIC microscope. WT haploid (A) and diploid (B) cells are shown for comparison. (C) No significant abnormalities were found in the Δ*cbf12* strain. By contrast, the cultures of the

Δ*cbf11* (D, F) and Δ*cbf11* Δ*cbf12* (E) strains are heterogeneous in shape and size of both cells and nuclei. Infrequently, cells display the 'cut' phenotype (asterisks), very large nuclei, pseudohyphal growth, multiple septa (arrowheads) or aberrantly thick septa (arrows).

4.1.4 Adhesion and flocculation tests

Our data on colony and cell morphology prompted us to test the effects of CSL genes deletions on cell adhesion. First, we performed washing assays (see Section 3.1.1.2) with spotted giant colonies of the respective deletion strains grown on YES plates. Cells bearing *cbf12*$^+$ deletion repeatedly showed decreased adhesion to the agar plate. Some cell mass of the WT and Δ*cbf11* spots remained attached to the surface, while the Δ*cbf12* and Δ*cbf11* Δ*cbf12* spots were washed off completely. This observation was documented microscopically (see Figure 4.11).

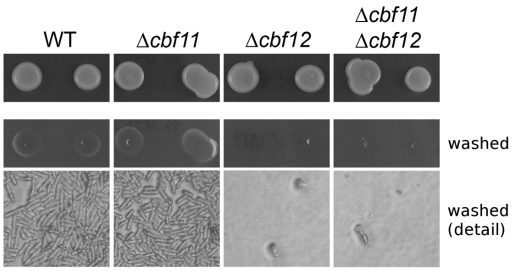

Figure 4.11 – Roles of *cbf11*$^+$ and *cbf12*$^+$ in cell adhesion. Cells were spotted on a YES plate, incubated in standard settings for 14 days, and then washed with a stream of water. A layer of cells remained adhering to the agar in case of the WT and Δ*cbf11* strains. On the contrary, strains lacking *cbf12*$^+$ were washed off completely. A microscopic picture of the washed surface is shown in the bottom panel.

Next, we studied the CSL genes effect on adhesion in liquid cultures (see Section 3.1.1.2). Overexpression of *cbf12*$^+$ in WT strain triggered flocculation (macroscopically visible cell aggregate formation) in a logarithmic-phase culture (see Figure 4.12A), while no flocculation was observed for the WT control. When the Δ*cbf11* deletion strain was tested, we observed a similar flocculation phenotype as in the *cbf12*$^+$ overexpressor strain (see Figure 4.12A). Only in this case cultures were left to grow to the stationary phase, which is generally more supportive of aggregation in yeasts (Straver *et al.*, 1993). Hence we conclude that Cbf11 acts as a negative regulator and Cbf12 as a positive regulator of cell adhesion in fission yeast.

While flocculation is predominantly mannose-dependent in *Saccharomyces cerevisiae* (Miki *et al.*, 1982), in *Schizosaccharomyces pombe* it was found to be mediated rather by galactosyl residues (Tanaka *et al.*, 1999). In accordance with that, using a sugar competition assay, we determined that flocculation induced by *cbf12*$^{+}$ overexpression could be abolished by the addition of galactose but not mannose to the cells (see Figure 4.12B). Since agar is a galactose polymer, it is likely that both the cell-cell and cell-agar surface adhesion properties affected by manipulation of the respective CSL genes are galactose-dependent.

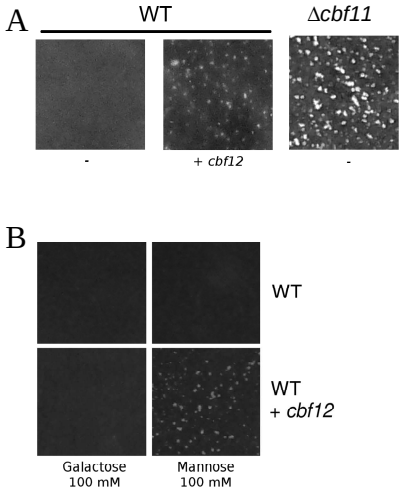

Figure 4.12 – Deletion of *cbf11*$^{+}$ or overexpression of *cbf12*$^{+}$ trigger flocculation. (A) Cells transformed with either an empty vector or a plasmid encoding *cbf12*$^{+}$ were grown in parallel in liquid inducing $MB_{\text{-ura-thiamin}}$ medium at 30°C. The overproduction of Cbf12 triggered flocculation. Δ*cbf11* cells were grown to stationary phase under the same conditions and displayed strong flocculation as well. (B) The Cbf12-induced flocculation is galactose-dependent, as confirmed by competition assays.

4.2 Quantitative real-time PCR analysis

Our initial hypothesis proposed a role for Cbf11 and Cbf12 in the regulation of transcription. So far, data concerning their subcellular localization, DNA binding and mutant phenotypes (Prevorovsky *et al.*, 2008) all support this assumption. However, the pleiotropy of the mutant phenotypes precludes a straight and precise determination of the CSL-regulated processes. A possible means to circumvent these obstacles is to perform a global transcriptome analysis of cells in which CSL expression was manipulated. Microarray experiments for two biological replicates were performed in collaboration with the laboratory of Dr. Jürg Bähler, Wellcome Trust Sanger Institute (Prevorovsky, unpublished data). See Table 4.2 for the list of strains used. Genes were considered differentially expressed when showing a twofold increase/decrease in mRNA levels relative to the control in both biological replicates.

Table 4.2 – Strains used for the microarray experiments.

Deletion		**Control**
Δ*cbf11* (CBF11 KO)	vs.	WT (PN559)
Δ*cbf12* (MP03)		
Δ*cbf11* Δ*cbf12* (MP09)		
Overexpression		**Control**
WT + *cbf11*$^{+}$ (PN559 + pJR08)	vs.	WT + vector (PN559 + pREP42MHN)
WT + *cbf12*$^{+}$ (PN559 + pMP32)		

On the basis of the microarray results, our data on adhesion/flocculation properties and spot test sensitivity/resistance responses, we selected genes of interest whose expression profiles were found to be significantly altered in comparison to control in the microarray analyses. We wanted to confirm these changes in an independent manner using a different method. Therefore we decided to use quantitative real-time reverse transcription PCR (qRT-PCR) to assess the mRNA levels of eleven genes, namely: *fip1*$^{+}$, *frp1*$^{+}$, *vht1*$^{+}$, *str1*$^{+}$, *str3*$^{+}$, SPBC947.05c, SPAC1F8.02c, which belong to iron regulon; and SPAC977.05c, SPCC1795.13, SPBC359.04c, SPBC1348.02, whose products may possibly play a role in adhesion of *Schizosaccharomyces pombe*

cells (see Table 4.3 for detailed information on the respective genes). As such, all the genes are relevant to our previous results. The *act1*$^+$ gene coding for the fission yeast actin was chosen as a normalisation control.

SPAC977.05c belongs to a conserved fungal family of genes that have recently undergone subtelomeric duplication. The family subsumes three genes, namely SPAC977.05c, SPBC1348.06c and SPBPB2B2.15. SPAC977.05c represents the whole family in the text. SPBC1348.02 is a member of a fission yeast specific 5Tm protein family that have been duplicated in subtelomeric region recently. The family includes four genes, namely SPBC1348.02, SPAC750.05c, SPBPB2B2.19c and SPAC977.01. SPBC1348.02 represents the whole family in the text.

The gene sequences within a family are theoretically but not practically distinguishable from each other in microarray or qRT-PCR experiments, making both methods comparable between each other in analysis of these genes.

Table 4.3 – Genes subjected to qRT-PCR analysis.

Gene	**Characteristics of product**	**Reference**
fip1$^+$	iron permease Fip1	(Pelletier *et al.*, 2002)
frp1$^+$	ferric-chelate reductase Frp1	(Pelletier *et al.*, 2002)
vht1$^+$	vitamin H transporter Vht1	(Stolz, 1999; Rustici *et al.*, 2007)
str1$^+$	siderophore-iron transporter Str1	(Pelletier *et al.*, 2002)
str3$^+$	siderophore-iron transporter Str3	(Pelletier *et al.*, 2002)
SPBC947.05c	ferric-chelate reductase (predicted)	(Rustici *et al.*, 2007)
SPAC1F8.02c	sequence orphan, *S. pombe* specific, GPI anchored, cell surface glycoprotein (predicted)	(Rustici *et al.*, 2007)
SPAC977.05c	conserved fungal family, zinc-ion binding, response to cadmium, subtelomeric duplication[a]	(Aslett and Wood, 2006; Matsuyama *et al.*, 2006; Chen *et al.*, 2003)
SPCC1795.13	sequence orphan, possibly *S. pombe* specific, GPI anchored, cell surface glycoprotein (predicted)	(De Groot *et al.*, 2003)
SPBC359.04c	cell surface glycoprotein (predicted), DIPSY family	(Linder and Gustafsson, 2008)
SPBC1348.02	*S. pombe* specific 5Tm protein family, subtelomeric duplication[b]	(Aslett and Wood, 2006; Matsuyama *et al.*, 2006)
act1$^+$	actin Act1, normalisation control	(Mertins and Gallwitz, 1987)

[a] SPAC977.05c represents a conserved fungal family of genes that have undergone a recent subtelomeric duplication. The family subsumes three genes, namely SPAC977.05c, SPBC1348.06c and SPBPB2B2.15.

[b] SPBC1348.02 represents a *Schizosaccharomyces pombe specific* 5Tm protein family that have been duplicated in subtelomeric region recently. The family includes four genes, namely SPBC1348.02, SPAC750.05c, SPBPB2B2.19c and SPAC977.01.

4.2.1 qRT-PCR setup verification

Several assumptions regarding the qRT-PCR experiments had to be tested prior to the expression analysis itself (see Section 3.3.4.2). For assessment of the mRNA levels in qRT-PCR experiment, the oligo(dT) primers in reverse transcription reactions are suitable. Using these primers allows for the 3' termini being reverse transcribed with high fidelity. Therefore, primer pairs were designed to amplify ~200 bp fragments close to the 3' termini of the target mRNAs (cDNAs). The primers were first tested in conventional colony PCR (see Section 3.3.4.1) to select the most suitable annealing temperature and to verify their specificity (see Figure 4.13).

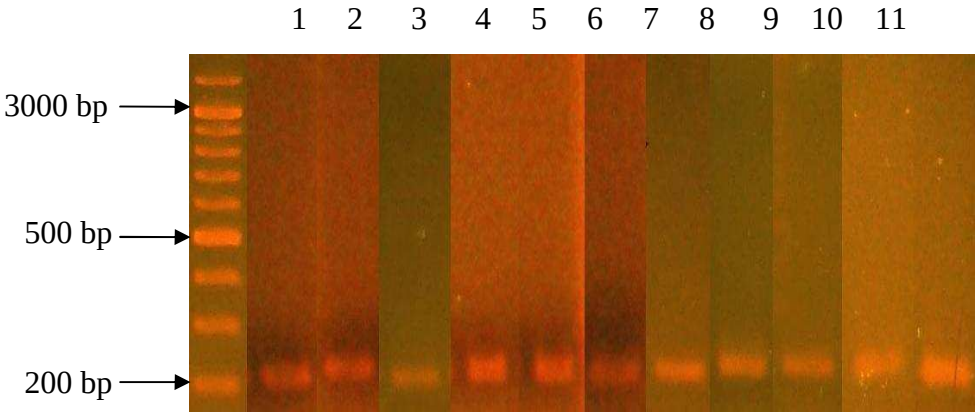

Figure 4.13 – Primer specificity verification. PCR amplification products were run on 2% agarose gel to assess their length. The respective products are shown from 1 to 11: *fip1*$^+$, *frp1*$^+$, *vht1*$^+$, *str1*$^+$, *str3*$^+$, SPBC947.05c, SPAC1F8.02c, SPAC977.05c, SPCC1795.13, SPBC359.04c and SPBC1348.02. The #SM0331 GeneRuler^{TM} DNA Ladder Mix from Fermentas was used as a marker.

Once this was accomplished, we proceeded to qRT-PCR calibration. To obtain reliable data, the PCR amplification efficiency for all of the respective genes analysed must be similar and close to 100% over a range of target cDNA concentrations (Livak and Schmittgen, 2001). In order to test these premises we subjected fourfold serial dilutions of the PN559 strain chromosomal DNA to the qPCR analysis. But for the least concentrated dilution (excluded from further calculations), the results were satisfactory, confirming a roughly 100% efficiency of the amplification reactions. The range of C_Ts measured corresponded to the range expected for the actual analysis of cDNAs (see Figure 4.14).

Next, we extracted RNA from exponentially growing culture of the PN559 strain and performed reverse transcription in standard settings and in mock settings (where no reverse transcriptase was added). With these products we executed qRT-PCR analysis, so as to assess genomic DNA contamination or, in other words, DNase treatment efficiency and to estimate the abundance of each mRNA tested. The results are presented in Figure 4.15. Reverse transcription reactions in mock settings all gave sufficiently low signals. Melting analysis of all reactions was run to attest that only one DNA species was amplified. Indeed, single fluorescence peaks were detected in melting analysis confirming that only the one desired PCR product had been present (see Figure 4.16).

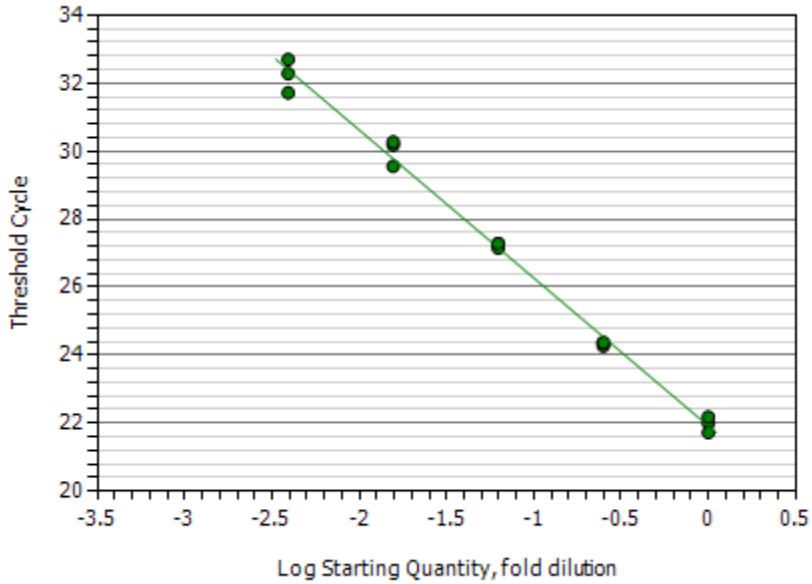

Figure 4.14 – An exemplary linear range assessment for SPAC977.05c.

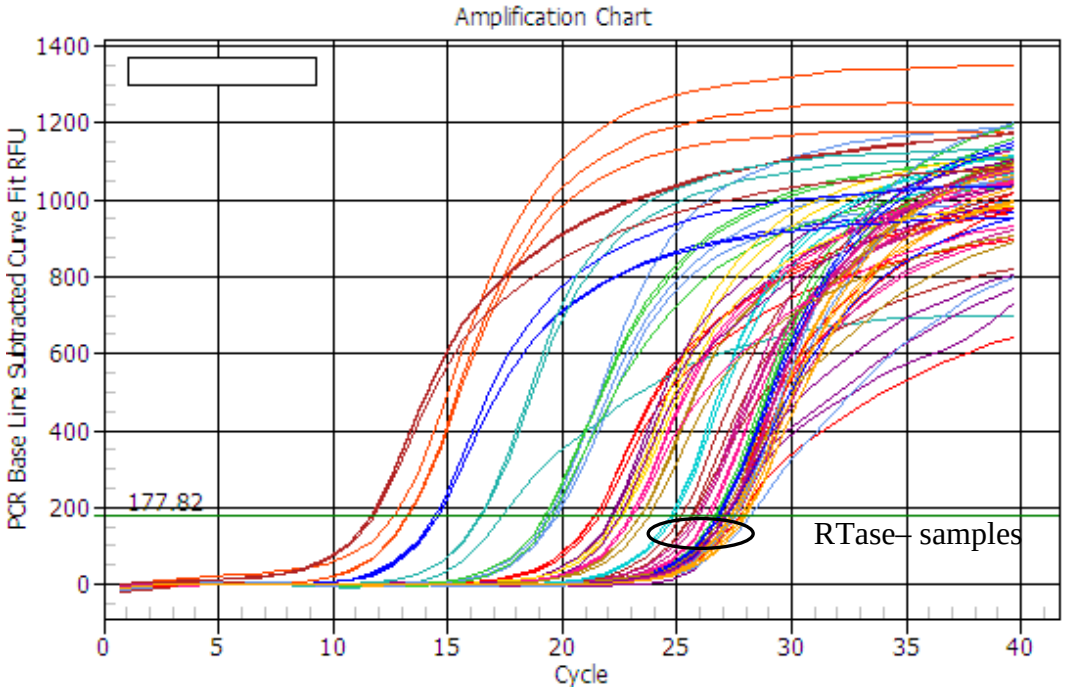

Figure 4.15 – Reverse transcription in standard settings and in mock settings, the latter are encircled and inscribed in the graph. The reactions in mock settings all gave sufficiently low signals. A rather prominent position of RTase– SPAC977.05c amplification curves (light blue) is caused by a recent duplication of these subtelomeric genes. Therefore, the primer pairs anneal to more than one site allowing for more template to be amplified. The proximity of some RTase+ amplification curves to the mock reaction signals is due to very low expression of the corresponding genes.

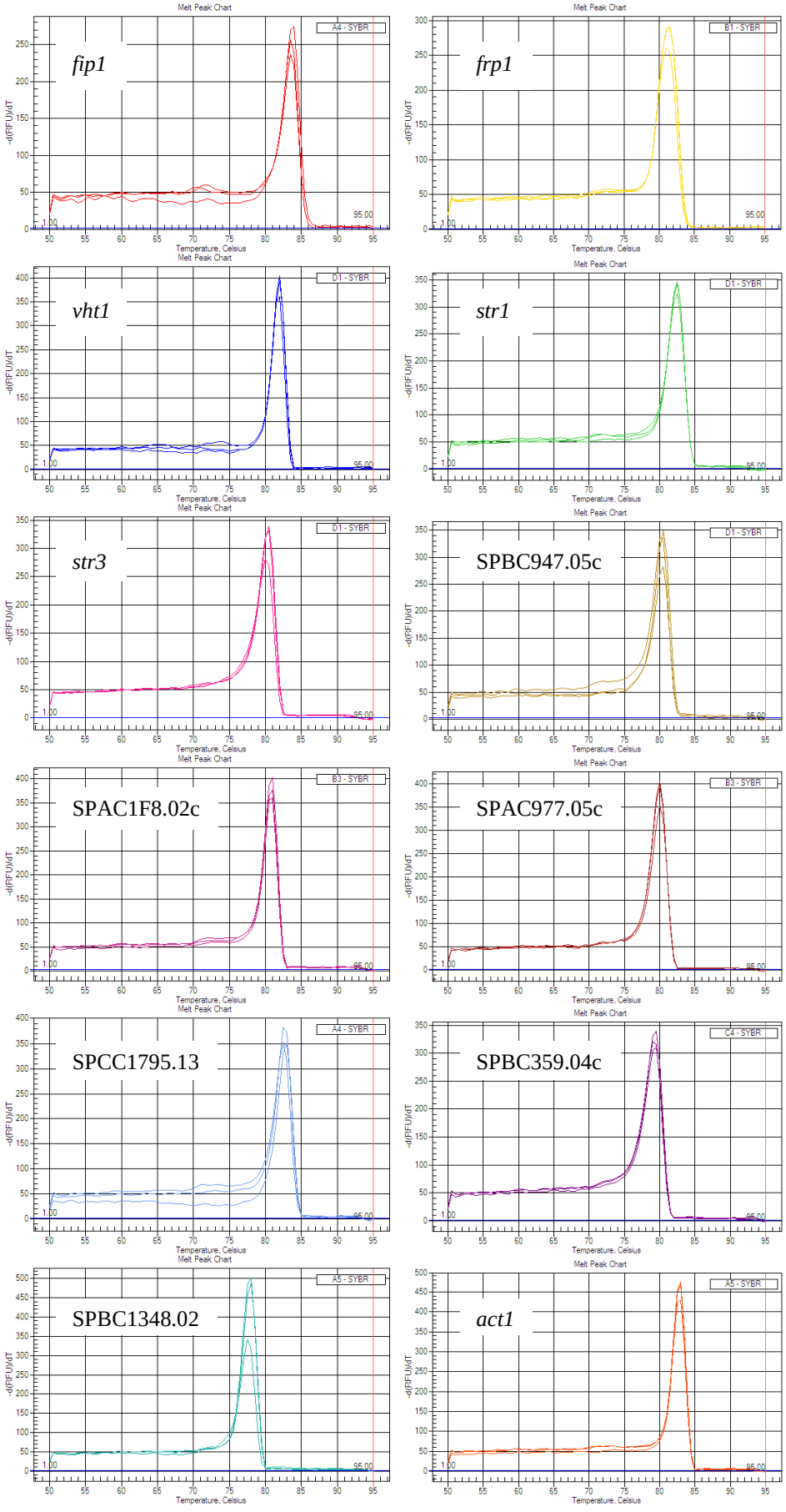

Figure 4.16 – Melting analysis of all samples shows a single peak for each pair of primers.

4.2.2 Experimental design

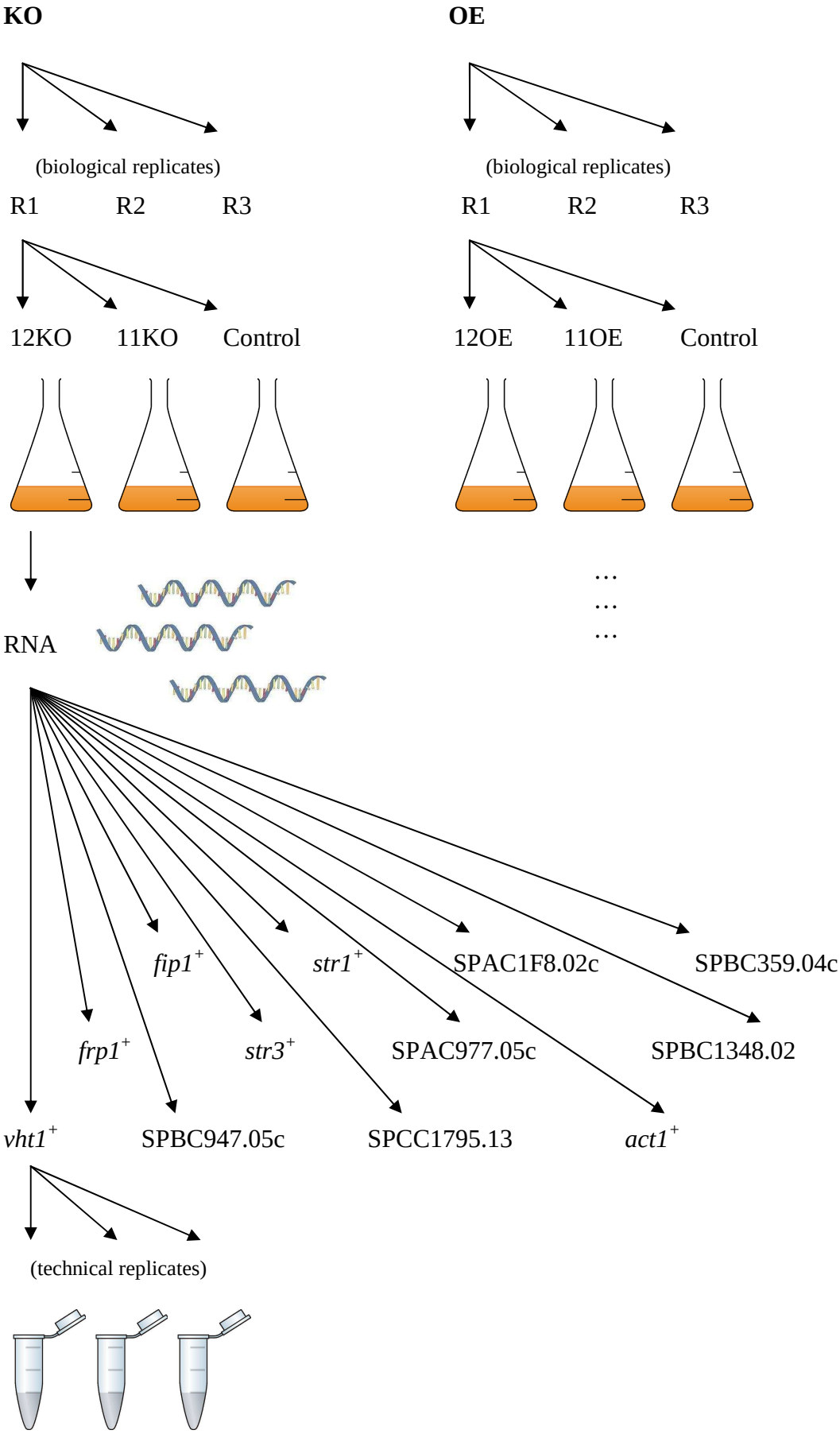

4.2.3 Expression analysis

Having passed all these tests successfully, we moved on to the actual cDNA levels analysis. We had two sets of strains to study (see Table 4.4) and performed three biological replicates for each of them. Cells for each biological replicate were cultivated in parallel, so as to minimise different external influences within the replicate that could affect our results. Prior to testing the overexpressor strains, the actual production of Cbf12 and Cbf11, respectively, was verified by western blotting (see Figure 4.17) for each of the three biological replicates.

Table 4.4 – Strains used for the qRT-PCR experiments.

Deletion		**Control**
Δ*cbf12* (MP03)	vs.	WT (PN559)
Δ*cbf11* (CBF11 KO)		
Overexpression		**Control**
WT + *cbf12*$^{+}$ (PN559 + pMP32)	vs.	WT + vector (PN559 + pREP42MHN)
WT + *cbf11*$^{+}$ (PN559 + pJR08)		

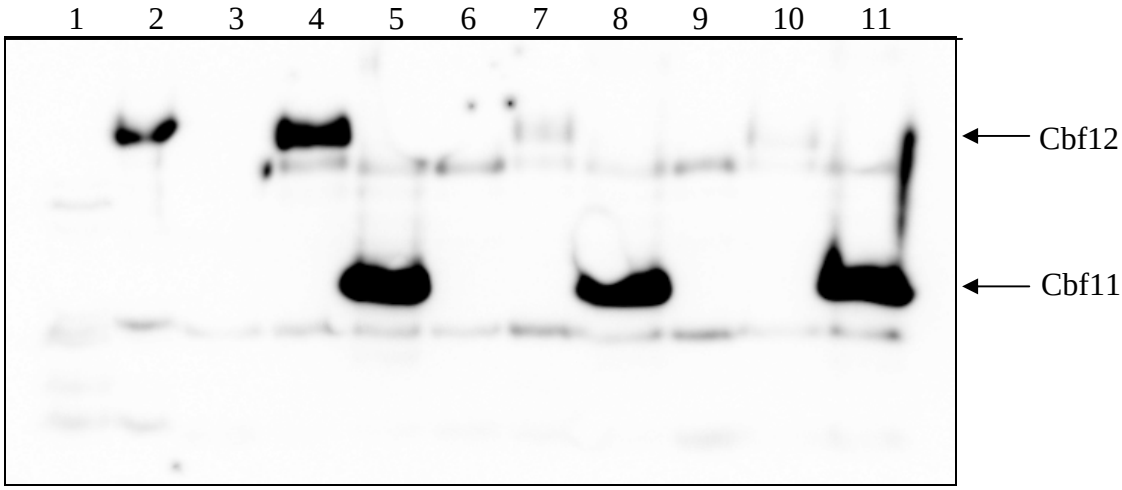

Figure 4.17 – Western analysis of HisMyc-tagged Cbf12 (pMP32, pREP42MHN backbone) and Cbf11 (pJR08, pREP42MHN backbone). Cultures were induced by the removal of thiamin from media. Lysate of WT + pREP42MHN (empty vector) was used as a negative control (line 1), lysate of WT + pMP32 as a positive control (line 2). Lines 3, 6, 9 – analysed samples of WT + pREP42MHN; 4, 7, 10 – analysed samples of WT + pMP32; lines 5, 8, 11 – analysed samples of WT + pJR08.

Next, qRT-PCR analyses of the three biological replicates for both the deletion and overexpressor sets of strains were performed. Raw data acquired were subjected to filtering, as described in Section 3.3.4.3. Our results are summarised in Figures 4.18-4.21 and Tables 4.5-4.6.

Figures 4.18 and 4.19 deal with the deletion set of strains. Figure 4.18 depicts the comparison of the respective genes to the endogenous reference (actin) within one strain. For the sake of clarity and obviousness, the one graph is shown at two different scales in order to visualise also genes with low expression values. Overall, the expression of all genes except for SPAC977.05c is rather low compared to the abundant actin.

Figure 4.19 displays comparison of the deletion strains with the WT control. The results are shown at a logarithmic scale as a fold expression change. Generally, the deletion of *cbf12*$^{+}$ does not cause any dramatic changes in the mRNA levels, which corresponds to the previous microarray output (Prevorovsky, unpublished data). On the contrary, the *cbf11*$^{+}$ deletion results in significant expression differences from the WT strain, especially concerning the genes belonging to iron regulon. The changes also correspond well with the microarray data and outline an explanation of the obvious resistance of Δ*cbf11* strains to excess dose of iron in media at the molecular level. See Table 4.5 for comparison of the microarray and the qRT-PCR outputs.

A

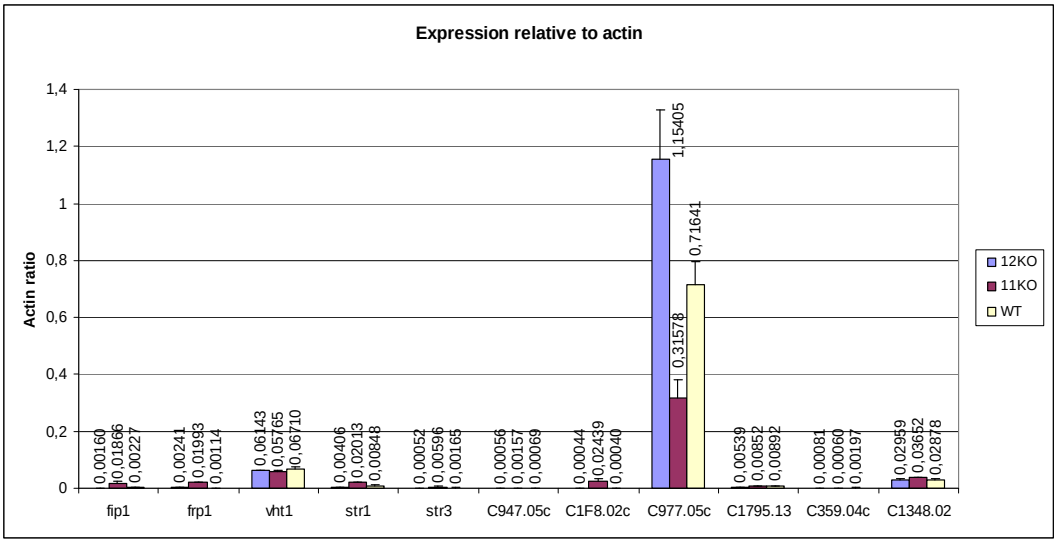

B

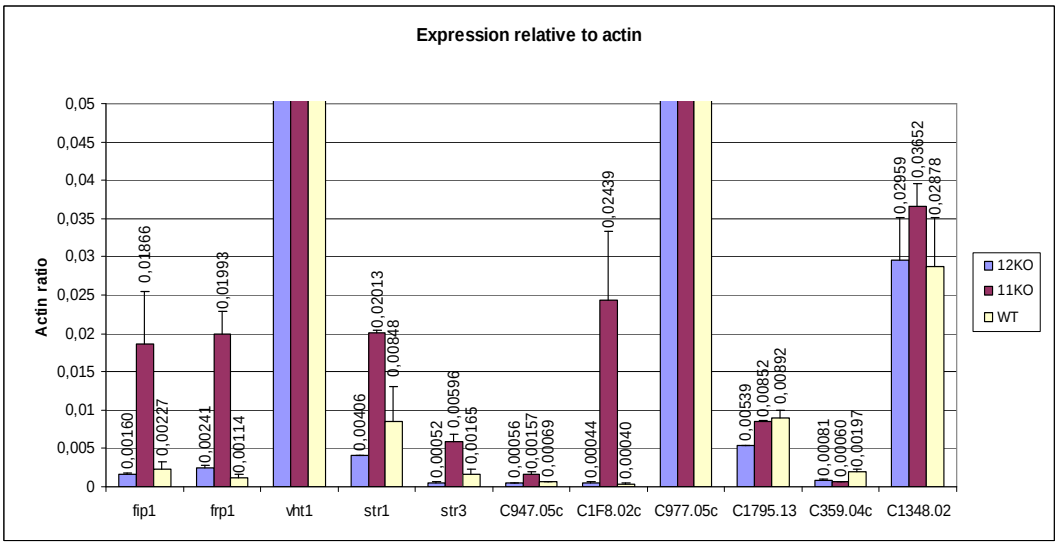

Figure 4.18 – Expression of each gene within one strain relative to actin, data shown for the deletion set of strains. (A) At the given scale, only SPAC977.05c of *cbf11*$^{+}$-lacking strain displays apparent difference. (B) The same results at a small scale exhibit changes also for *fip*$^{+}$, *frp*$^{+}$, *str1*$^{+}$, *str3*$^{+}$, SPBC947.05c, SPAC1F8.02c and SPBC359.04c in the strain lacking *cbf11*$^{+}$; and *frp*$^{+}$, *str3*$^{+}$ and SPBC359.04c in the strain lacking *cbf12*$^{+}$. For clarity reasons the first three letters (SPx) of the systematic names were omitted in the graph. The remaining tags are still unique and sufficient for unambiguous gene identification.

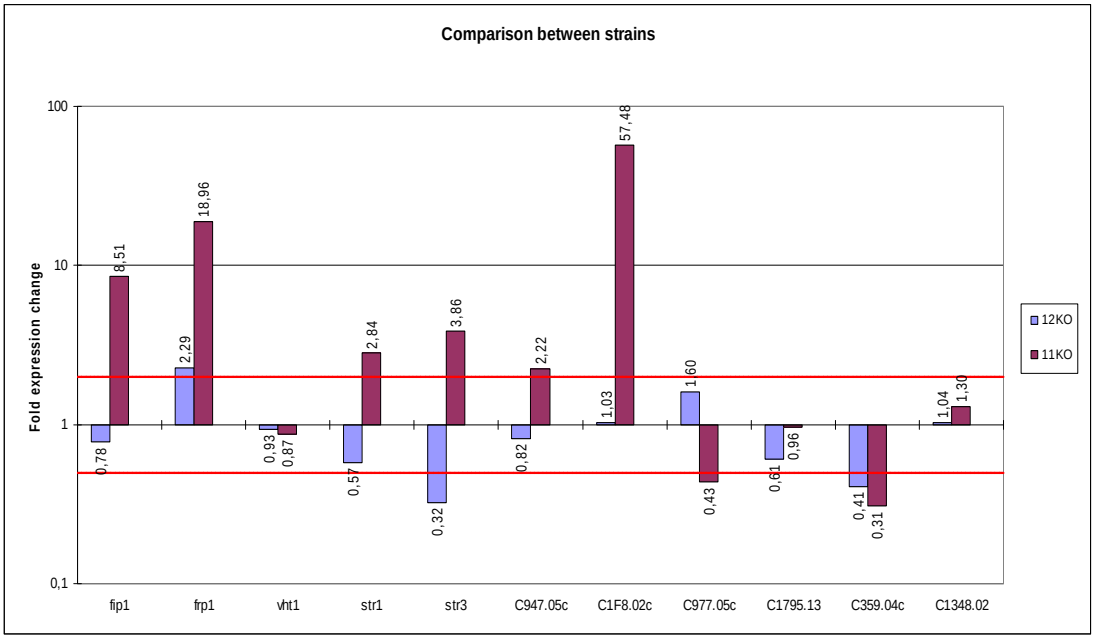

Figure 4.19 – Expression of each gene relative to control strain, data shown for the deletion set of strains at a logarithmic scale. The two red lines represent the thresholds of significant fold expression changes – twofold increase/decrease in mRNA levels relative to control. For clarity reasons the first three letters (SPx) of the systematic names were omitted in the graph. The remaining tags are still unique and sufficient for unambiguous gene identification.

The figures 4.20 and 4.21 display the results for the overexpressor set of strains. Figure 4.20 shows the abundance of the respective genes relative to the actin reference measure. Again, the one graph is presented at two different scales, so as to view the weakly expressed genes. Globally, all eleven genes manifest a rather moderate to low rate of expression when compared to that of actin. Note the different scale of Figures 4.18A and 4.20A.

Figure 4.21 depicts the fold change in expression of the respective overexpressor strains relative to the WT control. In this set, the excess dose of *cbf11*$^{+}$ does not result in any significant changes in expression, which observes the microarray data. SPAC977.05c represents the sole exception from this trend. On the other hand, the *cbf12*$^{+}$ overexpressor strain does exert considerable fold differences, most prominent of which are the genes coding for products with possible adhesive properties. These changes also correspond to the microarray pattern and support our previous results on adhesion and flocculation phenotypes at the molecular level. See Table 4.6 for comparison of the microarray and the qRT-PCR outputs. The high precise rates of fold expression change for SPAC977.05c may be caused by error of small values perhaps due to exceptionally low expression of this gene in the reference WT strain, thus causing overestimation of the result at least in the *cbf11*$^{+}$ overexpressor strain.

A

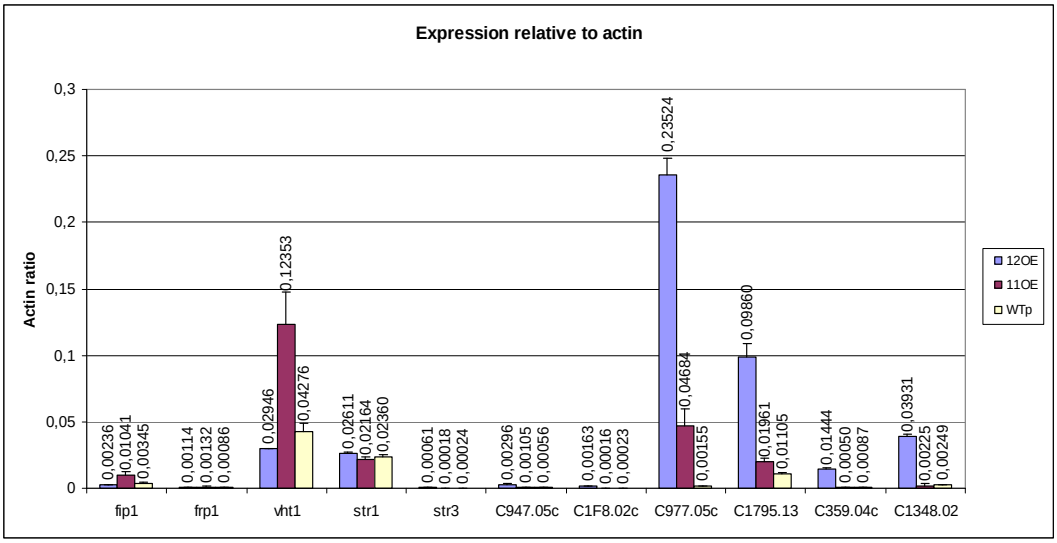

B

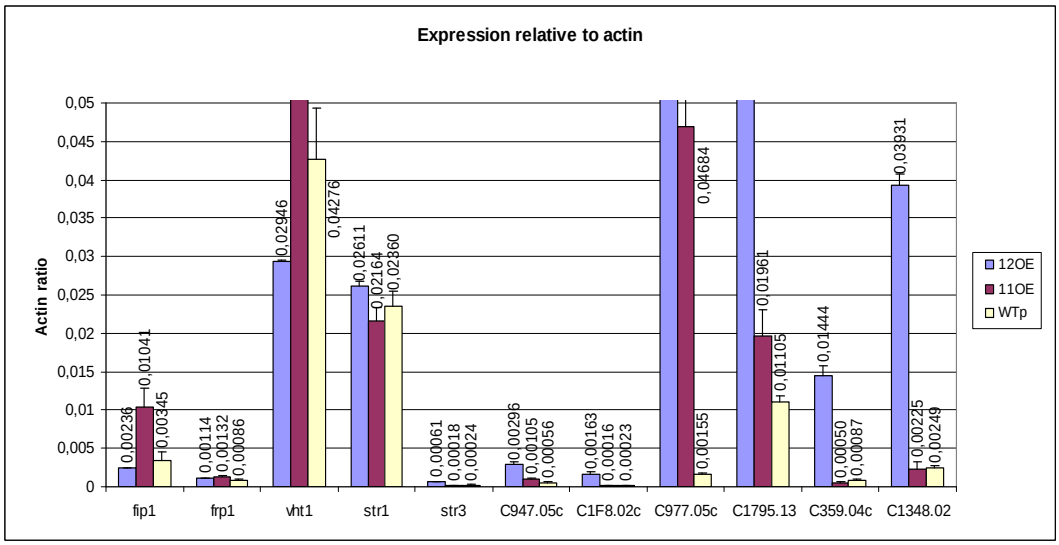

Figure 4.20 – Expression of each gene within one strain relative to actin, data shown for the overexpressor set of strains. (A) At the given scale, *fip1*$^{+}$, *vht1*$^{+}$ and SPAC977.05c display apparent difference in the strain overexpressing *cbf11*$^{+}$; and SPAC977.05c, SPCC1795.13, SPBC359.04c and SPBC1348.02 in the strain overexpressing *cbf12*$^{+}$. (B) While the same results at a small scale do not exhibit any more significant changes for the strain overexpressing *cbf11*$^{+}$, additional differences appears in the strain overexpressing *cbf12*$^{+}$ for *str3*$^{+}$, SPBC947.05c and SPAC1F8.02c. For clarity reasons the first three letters (SPx) of the systematic names were omitted in the graph. The remaining tags are still unique and sufficient for unambiguous gene identification.

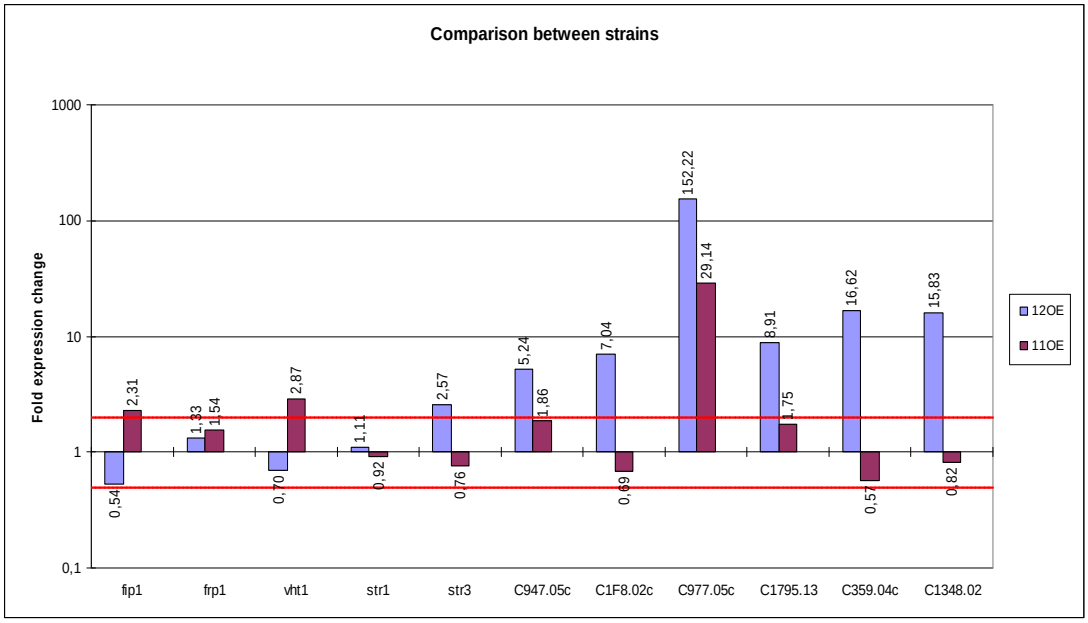

Figure 4.21 – Expression of each gene relative to control strain, data shown for the overexpressor set of strains at a logarithmic scale. The two red lines represent the thresholds of significant change – twofold increase/decrease in mRNA levels relative to control. For clarity reasons the first three letters (SPx) of the systematic names were omitted in the graph. The remaining tags are still unique and sufficient for unambiguous gene identification.

Table 4.5 – Comparison of the microarray and qRT-PCR fold expression change values for the corresponding gene and strain. Yellow fields indicate upregulation, blue areas indicate downregulation, gray ones mark insignificant expression changes of the respective genes.

12KO		Gene	11KO	
qRT-PCR	microarray		qRT-PCR	microarray
0.78	1.40	*fip1*$^+$	8.51	5.12
2.29	1.18	*frp1*$^+$	18.96	3.91
0.93	1.16	*vht1*$^+$	0.87	0.46
0.57	1.52	*str1*$^+$	2.84	5.62
0.32	0.97	*str3*$^+$	3.86	10.36
0.82	1.07	C947.05c	2.22	2.21
1.03	0.95	C1F8.02c	57.48	16.92
1.60	0.41	C977.05c	0.43	0.35
0.61	0.98	C1795.13	0.96	1.17
0.41	1.03	C359.04c	0.31	0.61
1.04	0.96	C1348.02	1.30	0.80

Table 4.6 – Comparison of the microarray and qRT-PCR values for the corresponding gene and strain. Yellow fields indicate upregulation, gray ones mark insignificant expression changes of the respective genes, black areas denote missing values. These genes were not included in the formulation of accordance between the two methods.

12OE		Gene	11OE	
qRT-PCR	microarray		qRT-PCR	microarray
0.54	1.67	*fip1*$^+$	2.31	3.14
1.33	1.20	*frp1*$^+$	1.54	1.03
0.70	2.02	*vht1*$^+$	2.87	2.23
1.11	1.44	*str1*$^+$	0.92	1.36
2.57	0.97	*str3*$^+$	0.76	
5.24	1.05	C947.05c	1.86	0.62
7.04	0.71	C1F8.02c	0.69	
152.22	8.02	C977.05c	29.14	1.51
8.91	6.09	C1795.13	1.75	0.91
16.62	25.53	C359.04c	0.57	1.31
15.83	11.71	C1348.02	0.82	1.24

Table 4.7 – Ratio of accordance between microarray and qRT-PCR results.

Deletion	**Agreement in results**
Δ*cbf12* (MP03)	63.6%
Δ*cbf11* (CBF11 KO)	81.8%
Overexpression	
WT + *cbf12*$^{+}$ (PN559 + pMP32)	63.6%
WT + *cbf11*$^{+}$ (PN559 + pJR08)	88.9%

To summarise, we have obtained good correlation between the data acquired with the microarray technique (Prevorovsky, unpublished data) and the qRT-PCR method for both the deletion and overexpressor strains (see Table 4.7). Concerning the dynamic range, the qRT-PCR method is generally considered more precise than the microarrays. Also, while there were only two biological replicates performed in the microarray experiment, three biological repeats were executed with qRT-PCR, which confers the results of the latter higher impact.

In conclusion, our data obtained with qRT-PCR observe the output of the microarray experiment and do correspond with the phenotypes described earlier.

5 *DISCUSSION*

5.1 CSL family in *Schizosaccharomyces pombe*

In contrast to the premise that the presence of CSL genes in the genome is a hallmark of metazoan organisms, members of this family have been identified in fission yeast and other fungi (Prevorovsky *et al.*, 2007). The current understanding of the CSL family function stems merely from metazoan models and is best characterised within their engagement in the Notch signalling pathway (Artavanis-Tsakonas *et al.*, 1999; Bray and Furriols, 2001; Pursglove and Mackay, 2005). Since fungi lack this pathway, it is clear that the CSL homologs play a role independent of the Notch signalling here. Moreover, the metazoan CSL proteins have recently been reported to act in a broader context than only the Notch-restricted network (Barolo *et al.*, 2000; Beres *et al.*, 2006; Koelzer and Klein, 2003). These pieces of information indicate that the metazoan and the newly described members of the CSL family share a common ancestral function in regulating gene expression, even though both their upstream contexts and regulated processes may differ.

Various approaches were used to address the function of the two CSL genes identified in *Schizosaccharomyces pombe* when analysing strains where the respective genes had been subjected to manipulation (either deletion, or overexpression). Sensitivity/resistance tests were employed; giant colonies and monocolonies were studied; cell morphology was assayed; adhesion/flocculation properties were investigated; and qRT-PCR experiment was performed in search of potential CSL-associated phenotype alterations. Other members of our team have employed further different methods (e.g. microarrays) whose outputs will be taken in for comparison and discussion. The pleiotropy of the phenotypes observed at the multicellular, cellular and molecular levels imply a more general regulatory role, likely in transcription, of which previous data on subcellular localisation, DNA binding characteristics, and other features are supportive (Prevorovsky *et al.*, 2008). Similar range of phenotypes was reported for mutants in other general transcription regulators, such as some components of the Mediator complex (Szilagyi *et al.*, 2002; Zilahi *et al.*, 2000).

5.1.1 Growth, sensitivity and resistance phenotypes

Our growth curve measurements revealed impairment in growth of strains harbouring deletion of *cbf11*$^+$, which phenotype was further accentuated in case of simultaneous deletion of *cbf12*$^+$. Such a result is suggestive of some cross-talk between Cbf11 and Cbf12. When preparing liquid cultures of the overexpressor strains for our qRT-PCR experiment we noticed an opposite phenotype in *cbf11*$^+$ overexpressor strain than that of the Δ*cbf11* strain – although the growth curves were not constructed, the *cbf11*$^+$ overexpressor strain obviously manifested faster growth than the WT transformed with an empty vector only. On the other hand, overexpression of *cbf12*$^+$ in a WT strain caused a strong impairment in growth. These data imply that Cbf11 may function as a positive regulator and Cbf12 as a negative regulator of fission yeast cells' growth.

The sensitivity/resistance spot tests performed showed similar growth impairment of Δ*cbf11* strains on solid rich media in 19°C, or containing 2.3% formamide, 11 mM caffeine, and 0.1 mM cadmium. In the case of cadmium present in the media the Δ*cbf11* strains exhibited impaired growth which effect was found to be accentuated by simultaneous deletion of *cbf12*$^+$. On the contrary, growth on solid media with 4 mM $FeCl_2$ added exerted resistance of the Δ*cbf11* strains with even higher tolerance to excess dose of iron in the case of simultaneous deletion of both CSL genes. The phenotypes observed on plates with cadmium and iron again imply cross-talk between the two proteins. These rather puzzling contradictory responses (sensitivity to cadmium and resistance to iron at the same time) to the two substances inducing oxidative stress conditions is likely caused by activation of different regulatory pathways (Chen *et al.*, 2008) since cadmium and iron cause distinct types of oxidative stress. It is noteworthy that no phenotype was observed when testing the third agent causing oxidative stress, H_2O_2. Even though a wide range of concentrations was assayed we did not find any difference between the strains. Later it was shown with confidence by another member of our team that Δ*cbf12* strains manifest sensitivity to H_2O_2. Our previous false negative results may have been caused by using a batch of H_2O_2 that had already decomposed. The third phenotype, distinct from the two previously described, does support the theory of diverse regulatory pathways being activated by substances inducing different types of oxidative stress. Taken together, the complexity of these data precludes

a straightforward interpretation of Cbf11 and Cbf12, respectively, in response to conditions of elevated oxidative stress, since the precise nature of the three substances' functioning remains unclear.

A phenotype, previously not observed while we were performing spot tests, occurred on solid media containing 11 mM caffeine. Here, h^+ and h^- counterparts were found not to be comparable. Instead, all four h^- strains manifested greater sensitivity than their h^+ partner strains. Taken separately, Δ*cbf11* strains in both the h^+ and h^- settings displayed sensitivity when confronted with their WT or Δ*cbf12* counterparts. The growth on solid media with 2.3% formamide added exerted a similar phenotype, although not absolutely. Δ*cbf11* strains generally exhibited growth impairment in comparison with WT or Δ*cbf12*. Except for Δ*cbf11* cells h^- strains showed increased sensitivity to formamide, which phenotype was most prominent in case of the h^- double deletion strain. Neither for caffeine, nor for formamide sensitivities is the reason known. We conclude that the manifestation of the phenotype is mating type-specific. The different responses of h^+ and h^- strains, respectively, must be determined by their distinct physiology and/or gene expression pattern. However, the exact mechanism of this effect is unknown and will be addressed in future studies, since it may be important for basic fission yeast biology.

In the work of Bimbó *et al.* (2005), strains with deletions of all kinases were prepared and subjected to a range of sensitivity/resistance tests, so as to determine their possible involvements in response to the respective stress inducing substances and processes they may regulate. A meaningful comparison of our observed phenotypes with those presented in the paper (Bimbó *et al.*, 2005) may have indicated the position of CSL proteins in the regulatory network. Since we did not find any phenotypes comparable to those observed and clustered by Bimbó *et al.* (2005), except for the protraction in growth of Δ*cbf11* strains at 19°C which by itself is insufficient, we turned to the microarray data acquired (Prevorovsky, unpublished data). A number of genes were differentially expressed which are associated with the uptake and metabolism of iron and biotin. As described above we did observe an iron-resistance phenotype in Δ*cbf11* strains (see the following section for details). Furthermore, as determined by a comparison of the microarray results to a database of expression profiles already existing (Bähler, unpublished data), there is a major overlap between the pattern of our strains and Mediator mutant strains Δ*sep10* (Δ*med31*) and *sep15-598* (*med8-598*) (Miklos *et al.*, 2008; Linder *et al.*, 2008).

These strains were reported to be sensitive to formamide, cadmium and caffeine. Indeed, we too found our deletion strains to manifest intolerance to the respective substances as described above. These similarities provide a link between the CSL proteins and the regulation of transcription.

5.1.2 Uptake of iron and biotin

There are two uptake routes for iron in *Schizosaccharomyces pombe*. In the reductive pathway, Fe^{3+} ions from the environment are first reduced to Fe^{2+} by the cell-surface reductase Frp1, then re-oxidized by the Fio1 oxidase, and imported into the cell by the Fip1 permease. The non-reductive pathway functions via the Str1, Str2 and Str3 transporters in the plasma membrane that recognise complexes of iron with the siderophore chelators. The genes encoding these uptake proteins are transcriptionally regulated by iron via the Fep1 transcription factor which acts as a repressor when iron is abundant (Labbe *et al.*, 2007). The list of Fep1/iron-regulated genes was recently determined (Rustici *et al.*, 2007) and overlaps significantly with the group of genes differentially regulated in Δ*cbf11* cells. One of these genes, the vitamin H (biotin) transporter *vht1*$^+$, is actually the only gene found to show reciprocal correlation in mRNA level with *cbf11*$^+$ deletion/overexpression. Such observations would suggest a role for CSL proteins in the regulation of iron homeostasis. Indeed, as described above we found Δ*cbf11* to be resistant to excess dose of iron. However, no physiological response was observed of either CSL mutant to biotin excess/starvation or iron starvation. Our qRT-PCR data correspond with the microarray output and the previously stated resistance phenotype of Δ*cbf11* cells, since all the genes belonging to iron regulon are significantly upregulated in Δ*cbf11* strains. However, the reciprocal correlation in *vht1*$^+$ mRNA levels with *cbf11*$^+$ deletion observed in the microarray experiment was not confirmed by the qRT-PCR analysis. The iron-regulated genes show altered expression levels also in the Mediator mutants described (Linder *et al.*, 2008; Miklos *et al.*, 2008), again pointing out the possible link between CSL family and the regulation of transcription. Notwithstanding our clues in this field, the overall picture still remains rather blurred and awaits further investigation.

5.1.3 Colony morphology and adhesion

We observed marked alterations in giant colonies and monocolonies of the Δ*cbf11* strains (a Δ*cbf11*-associated 'shiny' phenotype with giant colonies and irregular shape of monocolonies). Moreover, both Cbf11 and Cbf12 play a role in cell-cell and cell-surface adhesion. Cbf11 acts as a negative regulator of adhesion, while Cbf12 functions as a positive regulator. It was previously described that changes in adhesive properties of cells have profound impact on yeast colony morphology (Nguyen *et al.*, 2004; Reynolds and Fink, 2001; Vopalenska *et al.*, 2005). Hence, a possible reason for the colony morphology aberrations of the Δ*cbf11* strains may be evoked by the increased adherence and/or the production of an extracellular 'shiny' material. A different but also plausible cause of the dissimilarities in Δ*cbf11* colonies may be cell morphology alterations due to separation defects manifested by a fraction of the cells in Δ*cbf11* colonies, as described earlier in other fungi (Vopalenska *et al.*, 2005; Voth *et al.*, 2005). Nonetheless, one explanation is not exclusive of the other (and *vice versa*) and the effects may combine.

On the molecular level, the microarray data are supportive of our results in this field, since several described or predicted adhesins and cell-surface glycoproteins (Linder and Gustafsson, 2008) showed significant increase in expression. E.g. the deletion of $cbf11^{+}$ resulted in 17-fold upregulation of the SPAC1F8.02c predicted GPI-anchored glycoprotein, and the overexpression of $cbf12^{+}$ induced 25-fold and 6-fold upregulation of the SPBC359.04c and SPCC1795.13 adhesins, respectively. Interestingly, these two genes were reported to be negatively regulated by the Cdk8 (Linder *et al.*, 2008), a subunit of the Mediator complex (Bjorklund and Gustafsson, 2005), the mutants of which are hyperflocculent (Watson and Davey, 1998). Our qRT-PCR output does observe the microarray results, since there is a great increase in expression of SPAC1F8.02c in the $cbf11^{+}$-lacking strains (57-fold upregulation), and every studied gene encoding a possible adhesin product shows marked upregulation in the $cbf12^{+}$ overexpressor strain.

5.1.4 Cell separation defects and diploidisation

When the expression of CSL genes was drawn off physiological levels, various cell separation defects occurred (in case of $cbf11^{+}$ deletion or $cbf12^{+}$ overexpression) that could generally be described as results of a failure in coordination of cellular and

nuclear division. These phenotypes subsumed multiple septation not followed by cellular division consequently causing pseudohyphal growth and formation of unusually thick septa. Rarely, large uninucleate cells with several septa were observed. In the WT control such defects were hardly ever seen. The above stated phenotypes resemble those of the so-called 'sep' mutants which are usually sterile and exhibit impaired response to stress inducing substances (Grallert *et al.*, 1999; Sipiczki *et al.*, 1993). Some of the 'sep' mutations have been reported to reside in genes coding for regulators of transcription (Ribar *et al.*, 1997; Szilagyi *et al.*, 2002; Zilahi *et al.*, 2000). Given the variety of phenotypes observed in these mutants, such results were not surprising. Two prominent examples are *sep10*$^{+}$ and *sep15*$^{+}$ coding for the subunits of the RNA polymerase II Mediator, Med31 and Med8, respectively. A significant overlap of our microarray data (Δ*cbf11* and overexpression of both *cbf11*$^{+}$ and *cbf12*$^{+}$) and the expression profiles of Δ*sep10* and *sep15-598* mutants was found, confirming the similarity at the molecular level as well. Moreover, there are physiological and also molecular similarities between our CSL mutants and strains lacking Cdk8, another Mediator component as described in Section 5.1.3 (Linder *et al.*, 2008), although the overlap of the respective microarray profiles is only minor. Hence we assume that some interaction between the CSL proteins and the Mediator likely takes place whose precise nature remains unclear.

Three main mechanisms of diploidisation were described. First, a bypass of M-phase may occur (Hayles *et al.*, 1994); second, multiple S-phases may take place (Jallepalli *et al.*, 1998; Kominami and Toda, 1997); and third, the M-phase may remain incomplete (Hirano *et al.*, 1986). All these events result in the so-called endoreduplication of the genome, thus increasing the ploidy of the affected cells. The diploidisation we observed in Δ*cbf11* and *cbf12*$^{+}$ overexpressor (Prevorovsky *et al.*, 2008) strains is probably closely related to the separation defects. Diploid subpopulations manifested as dark staining sectors in monocolonies cultivated on rich media containing phloxin B, as a diploid fraction observed by FACS and as large cells with oversize nuclei seen under a microscope. A number of mutations, mostly in genes involved in the cell cycle regulation and progression, were shown to increase the so-called endoreduplication or re-replication frequency. Hence, the respective mutant populations contain varying fractions of diploid or even polyploid cells. In case of our deletion/overexpressor strains an incomplete M-phase occurs due to lack of coordination between cellular and nuclear division, thus resulting in the

'cut' phenotype (Hirano *et al.*, 1986). Here, the prematurely formed septum either cuts the undivided nucleus inevitably resulting in death of such a cell, or misses the nucleus giving rise to a diploid and an anucleate compartment. If the cell division follows a stable (since it is homozygous in the mating locus, it is incapable of sporulation) diploid cell may then start a clonal diploid subpopulation. We have observed the 'cut' phenotype in association with the deletion of *cbf11*$^{+}$, the highest incidence being 22,8% in the double deletion strain (Prevorovsky *et al.*, 2008). The expression of *cut6*$^{+}$, encoding an acetyl coenzyme A carboxylase, of which the conditional mutant is 'cut', was decreased in both the Δ*cbf11* and the double deletion strains. However, this reason does not explain the diploid fraction in *cbf12*$^{+}$ overexpressor strain, since very few 'cut' cells were seen and the *cut6*$^{+}$ expression was not significantly altered. It is therefore likely that other mechanisms (possibly shared by Δ*cbf11* and *cbf12*$^{+}$ overexpressor) are responsible for the formation of diploid subpopulations in strains where the CSL genes had been manipulated. Our experiments have certainly affirmed a requirement for the CSL family in the maintenance of the fission yeast genome ploidy.

5.2 Cbf11 and Cbf12 as novel transcription factors

The two fission yeast CSL proteins display a number of features typical of transcription factors. They share domain composition and sequence motifs with the metazoan CSL family members (Prevorovsky *et al.*, 2007) and localise to the nucleus. While the binding characteristics of Cbf12 remain to be determined precisely, Cbf11 was found to specifically recognize and bind directly to the canonical CSL response element on DNA (Tun *et al.*, 1994). Moreover, the phenotypes observed for our deletion/overexpressor strains overlap with those of Mediator mutants at both the physiological and molecular level. Taking together all available clues from different parts of the fission yeast CSL project, we propose a role for Cbf11 and Cbf12 as novel fission yeast transcription factors which regulate or attune a number of processes. Since they function within a unicellular organism, their regulatory involvements obviously differ from those of their metazoan counterparts. Cbf11 and Cbf12 seem to regulate extracellular material production, colony morphology, cell adhesion, septation, coordination of nuclear and cellular division, and maintenance of genome ploidy.

For all our phenotypic results observed, the two paralogs function in a contradictory manner – Cbf11 consistently acts as a negative and Cbf12 as a positive regulator of the same processes (see Figure 5.1). Hence, a conclusion may be suggested that negative regulation mediated by Cbf11 might be the default state of CSL responsive genes in *Schizosaccharomyces pombe,* and Cbf12 might serve as their activator upon requirement which behaviour would be reminiscent of their metazoan CSL homologs (Hsieh *et al.*, 1996; Zhou *et al.*, 2000).

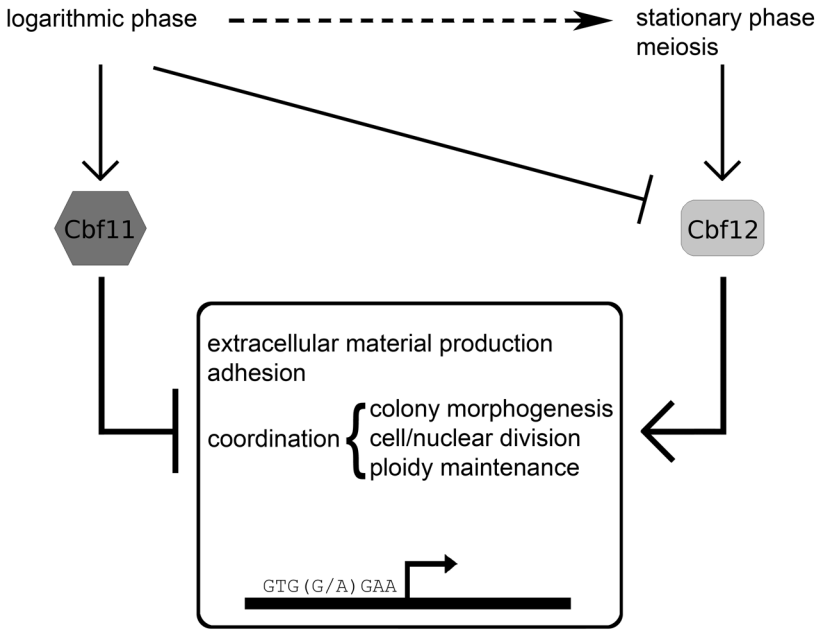

Figure 5.1 – A proposed model of CSL functioning in *Schizosaccharomyces pombe*. In log-phase vegetative cells Cbf11 is bound to CSL responsive promoters containing the GTG(G/A)GAA recognition sequence, and mediates their repression. Cbf12 is expressed at low levels under these conditions and cannot overcome the effect of Cbf11. Upon entry into the stationary phase of growth (high cell density, depleted nutrients), the Cbf12 protein levels rise and trigger the activation of the CSL target genes, e.g. by cancelling the effect of Cbf11 or by replacing Cbf11 at the respective promoters. The target genes are involved in processes such as extracellular material production, colony morphology establishment, cell adhesion, cellular and nuclear division and their coordination, and maintenance of genome ploidy. These genes seem to include several transcription factors, thus some apparently CSL-responsive genes may actually be regulated indirectly, by proteins downstream of Cbf11/Cbf12. At any time, a proper balance between the Cbf11 and Cbf12 levels and activities seems to be important for the above-mentioned processes not to be perturbed.

6 *CONCLUSIONS*

- In this study, we phenotypically characterised *Schizosaccharomyces pombe* strains harbouring deletions of *cbf11*$^+$ and *cbf12*$^+$, respectively. We analysed single deletion strains and strains with combined deletion of both CSL genes. Overexpressor strains with WT genetic background were constructed and subjected to analysis as well.

- So as to determine the function of CSL genes in Notch-less fungal settings, we assayed the mutant strains using various approaches: sensitivity/resistance tests were employed; giant colonies and monocolonies were studied; cell morphology was assayed; adhesion/flocculation properties were investigated; and qRT-PCR experiment was performed.

- We have shown that strains harbouring the deletion of *cbf11*$^+$ have impaired growth, overproduce 'shiny' extracellular material, are cold-sensitive, manifest intolerance to formamide, cadmium and caffeine, exhibit resistance to iron chloride, and have altered colony morphology.

- Either the deletion of *cbf11*$^+$ or overexpression of *cbf12*$^+$ result in increased cell adhesion, various cell separation defects (multiple septa, aberrantly thick septa, pseudohyphal growth; 'cut' phenotype in *Δcbf11* cells only), and high incidence of stable diploid formation in heterothallic strains.

- On the molecular level, microarray data are supportive of the phenotypes described above. We introduced the qRT-PCR method and by these means confirmed the microarray data for selected genes in an independent manner.

- The hypothesis was postulated, that Cbf11 and Cbf12 are transcription factors of *Schizosaccharomyces pombe* with contradicting, repressive and activating effects on target gene expression, respectively.

7 REFERENCES

1. Artavanis-Tsakonas, S., Rand, M. D., and Lake, R. J. (1999) Notch signaling: cell fate control and signal integration in development. *Science* **284:** 770-776.

2. Aslett, M. and Wood, V. (2006) Gene Ontology annotation status of the fission yeast genome: preliminary coverage approaches 100%. *Yeast* **23:** 913-919.

3. Bahler, J., Wu, J. Q., Longtine, M. S., Shah, N. G., McKenzie, A., III, Steever, A. B., Wach, A., Philippsen, P., and Pringle, J. R. (1998) Heterologous modules for efficient and versatile PCR-based gene targeting in *Schizosaccharomyces pombe*. *Yeast* **14:** 943-951.

4. Barolo, S., Walker, R. G., Polyanovsky, A. D., Freschi, G., Keil, T., and Posakony, J. W. (2000) A notch-independent activity of suppressor of hairless is required for normal mechanoreceptor physiology. *Cell* **103:** 957-969.

5. Basi, G., Schmid, E., and Maundrell, K. (1993) TATA box mutations in the *Schizosaccharomyces pombe* nmt1 promoter affect transcription efficiency but not the transcription start point or thiamine repressibility. *Gene* **123:** 131-136.

6. Beres, T. M., Masui, T., Swift, G. H., Shi, L., Henke, R. M., and MacDonald, R. J. (2006) PTF1 is an organ-specific and Notch-independent basic helix-loop-helix complex containing the mammalian Suppressor of Hairless (RBP-J) or its paralogue, RBP-L. *Mol Cell Biol* **26:** 117-130.

7. Bimbó, A., Jia, Y., Poh, S. L., Karuturi, R. K., den Elzen, N., Peng, X., Zheng, L., O´Connell, M., Liu, E. T., Balasubramanian, M. K., Liu, J. (2005) Systematic deletion analysis of fission yeast protein kinases. *Eukaryot Cell* **4**: 799-813.

8. Birnboim, H. C. and Doly, J. (1979) A rapid alkaline extraction procedure for screening recombinant plasmid DNA. *Nucleic Acids Res* **7:** 1513-1523.

9. Bjorklund, S. and Gustafsson, C. M. (2005) The yeast Mediator complex and its regulation. *Trends Biochem Sci* **30:** 240-244.

10. Bony, M., Thines-Sempoux, D., Barre, P., and Blondin, B. (1997) Localization and cell surface anchoring of the *Saccharomyces cerevisiae* flocculation protein Flo1p. *J Bacteriol* **179**: 4929–4936.

11. Bray, S. and Furriols, M. (2001) Notch pathway: making sense of suppressor of hairless. *Curr Biol* **11:** R217-R221.

12. Bray, S. J. (2006) Notch signalling: a simple pathway becomes complex. *Nat Rev Mol Cell Biol* **7:** 678-689.

13. Cappellaro, C., Baldermann, C., Rachel, R., and Tanner., W. (1994) Mating type-specific cell-cell recognition of *Saccharomyces cerevisiae*: cell wall attachment and active sites of a- and alpha-agglutinin. *EMBO J* **13:** 4737–4744.

14. Chen, D., Wilkinson, C. R., Watt, S., Penkett, C. J., Toone, W. M., Jones, N., Bähler, J. (2008) Multiple pathways diferentially regulate global oxidative stress responses in fission yeast. *Mol Biol Cell* **19**: 308-317

15. Chung, C. N., Hamaguchi, Y., Honjo, T., and Kawaichi, M. (1994) Site-directed mutagenesis study on DNA binding regions of the mouse homologue of Suppressor of Hairless, RBP-J kappa. *Nucleic Acids Res* **22:** 2938-2944.

16. Craven, R. A., Griffiths, D. J., Sheldrick, K. S., Randall, R. E., Hagan, I. M., and Carr, A. M. (1998) Vectors for the expression of tagged proteins in *Schizosaccharomyces pombe*. *Gene* **221:** 59-68.

17. Cutler, N. S., Pan, X., Heitman, J., and Cardenas, M. E. (2001) The TOR signal transduction cascade controls cellular differentiation in response to nutrients. *Mol Biol Cell* **12:** 4103–4113.

18. Decottignies, A., Sanchez-Perez, I., and Nurse, P. (2003) *Schizosaccharomyces pombe* essential genes: a pilot study. *Genome Res* **13:** 399-406.

19. De Groot, P. W., Hellingwerf, K. J., and Klis, F. M. (2003) Genome-wide identification of fungal GPI proteins. *Yeast* **20**: 781-796

20. De Las Penas, A., Pan, S. J., Castano, I., Alder, J., Cregg, R., and Cormack, B. P. (2003) Virulence-related surface glycoproteins in the yeast patogen *Candida glabrata* are encoded in subtelomeric clusters and subject to RAP1- and SIR-dependent transcriptional silencing. *Genes Dev* **17:** 2245–2258.

21. Domergue, R., Castano, I., De Las Penas, A., Zupancic, M., Lockatell, V., Hebel, R. J., Johnson, D., Cormack, B. P. (2005) Nicotinic acid limitation regulates silencing of *Candida* adhesins during UTI. *Science* **308:** 866–870.

22. van Dyk, D., Pretorius, I. S., and Bauer, F. F. (2005) Mss11p is a central element of the regulatory network that controls *FLO11* expression and invasive growth in *Saccharomyces cerevisiae*. *Genetics* **169:** 91–106.

23. Egel, R. (Ed.) (2004) The Molecular Biology of *Schizosaccharomyces pombe* - Genetics, Genomics and Beyond. Springer-Verlag Berlin Heidelberg New York.

24. Eisenhaber, B., Schneider, G., Wildpaner, M., Eisenhaber, F. (2004) A sensitive predictor for potential GPI lipid modification sites in fungal protein sequences and its application to genome-wide studies for *Aspergillus nidulans, Candida albicans, Neurospora crassa, Saccharomyces cerevisiae* and *Schizosaccharomyces pombe*. *J Mol Biol* **337:** 243–253.

25. Forsburg, S. L. (2003) *S. pombe* strain maintenance and media. *Curr Protoc Mol Biol* **Chapter 13:** Unit 13.15.

26. Frieman, M.B., McCaffery, J.M., and Cormack, B.P. (2002) Modular domain structure in the *Candida glabrata* adhesion Epa1p, a beta1,6 glucan-cross-linked cell wall protein. *Mol Microbiol* **46**: 479–492.

27. Frieman, M. B., and Cormack, B. P. (2003) The omega-site sequence of glycosylphosphatidylinositol-anchored proteins in *Saccharomyces cerevisiae* can determine distribution between the membrane and the cell wall. *Mol Microbiol* **50:** 883–896.

28. Frieman, M. B., and Cormack, B. P. (2004) Multiple sequence signals determine the distribution of glycosylphosphatidylinositol proteins between the plasma membrane and cell wall in *Saccharomyces cerevisiae*. *Microbiology* **150:** 3105–3114.

29. Gagiano, M., Bauer, F. F., and Pretorius, I. S. (2002) The sensing of nutritional status and the relationship to filamentous growth in *Saccharomyces cerevisiae*. *FEMS Yeast Res* **2:** 433–470.

30. Gatti, E., Popolo, L., Vai, M., Rota, N., and Alberghina, L. (1994) O-linked oligosaccharides in yeast glycosylphosphatidylinositol-anchored protein gp115 are clustered in a serine-rich region not essential for its function. *J Biol Chem* **69:** 19695–19700.

31. Gimeno, C. J., and Fink, G. R. (1994) Induction of pseudohyphal growth by overexpression of PHD1, a *Saccharomyces cerevisiae* gene related to transcriptional regulators of fungal development. *Mol Cell Biol* **14:** 2100–2112.

32. Grallert, A., Grallert, B., Zilahi, E., Szilagyi, Z., and Sipiczki, M. (1999) Eleven novel sep genes of *Schizosaccharomyces pombe* required for efficient cell separation and sexual differentiation. *Yeast* **15:** 669-686.

33. Gregan, J., Rabitsch, P. K., Sakem, B., Csutak, O., Latypov, V., Lehmann, E., Kohli, J., and Nasmyth, K. (2005) Novel genes required for meiotic chromosome segregation are identified by a high-throughput knockout screen in fission yeast. *Curr Biol* **15:** 1663-1669.

34. Guldal, C. G. and Broach, J. (2006) Assay for adhesion and agar invasion in *S. cerevisiae*. *J Vis Exp* **1**: 64.

35. Guo, B., Styles, C. A., Feng, Q., and Fink, G. (2000) A *Saccharomyces* gene family involved in invasive growth, cell-cell adhesion, and mating. *Proc Natl Acad Sci USA* **97:** 12158–12163.

36. Halme, A., Bumgarner, S., Styles, C. A., and Fink, G. R. (2004) Genetic and epigenetic regulation of the *FLO* gene family generates cell-surface variation in yeast. *Cell* **116:** 405–415.

37. Hamaguchi, Y., Matsunami, N., Yamamoto, Y., and Honjo, T. (1989) Purification and characterization of a protein that binds to the recombination signal sequence of the immunoglobulin J kappa segment. *Nucleic Acids Res* **17:** 9015-9026.

38. Hayles, J., Fisher, D., Woollard, A., and Nurse, P. (1994) Temporal order of S phase and mitosis in fission yeast is determined by the state of the p34cdc2-mitotic B cyclin complex. *Cell* **78:** 813-822.

39. Hedges, S. B. (2002) The origin and evolution of model organisms. *Nat Rev Genet* **3:** 838-849.

40. Henkel, T., Ling, P. D., Hayward, S. D., and Peterson, M. G. (1994) Mediation of Epstein-Barr virus EBNA2 transactivation by recombination signal-binding protein J kappa. *Science* **265:** 92-95.

41. Hertz-Fowler, C., Peacock, C. S., Wood, V., Aslett, M., Kerhornou, A., Mooney, P., Tivey, A., Berriman, M., Hall, N., Rutherford, K., Parkhill, J., Ivens, A. C., Rajandream, M. A., and Barrell, B. (2004) GeneDB: a resource for prokaryotic and eukaryotic organisms. *Nucleic Acids Res* **32:** D339-D343.

42. Hirano, T., Funahashi, S. I., Uemura, T., and Yanagida, M. (1986) Isolation and characterization of *Schizosaccharomyces pombe* cut mutants that block nuclear division but not cytokinesis. *EMBO J* **5:** 2973-2979.

43. Hoffman, C. S. and Winston, F. (1987) A ten-minute DNA preparation from yeast efficiently releases autonomous plasmids for transformation of Escherichia coli. *Gene* **57**: 267-272.

44. Honjo, T. (1996) The shortest path from the surface to the nucleus: RBP-J kappa/Su(H) transcription factor. *Genes Cells* **1:** 1-9.

45. Hsieh, J. J., Henkel, T., Salmon, P., Robey, E., Peterson, M. G., and Hayward, S. D. (1996) Truncated mammalian Notch1 activates CBF1/RBPJk-repressed genes by a mechanism resembling that of Epstein-Barr virus EBNA2. *Mol Cell Biol* **16:** 952-959.

46. Huang, G., Zhang, M., and Erdman, S. E. (2003) Posttranslational modifications required for cell surface localization and function of the fungal adhesin Aga1p. *Eukaryot Cell* **2:** 1099–1114.

47. Iraqui, I., Garcia-Sanchez, S., Aubert, S., Dromer, F., Ghigo, J. M., d'Enfert, C., and Janbon, G. (2005) The Yak1p kinase controls expression of adhesins and biofilm formation in *Candida glabrata* in a Sir4p-dependent pathway. *Mol Microbiol* **55:** 1259–1271.

48. Jallepalli, P. V., Tien, D., and Kelly, T. J. (1998) sud1(+) targets cyclin-dependent kinase-phosphorylated Cdc18 and Rum1 proteins for degradation and stops unwanted diploidization in fission yeast. *Proc Natl Acad Sci U S A* **95:** 8159-8164.

49. Jentoft, N. (1990) Why are proteins O-glycosylated? *Trends Biochem Sci* **15:** 291–294.

50. Kang, S., and Choi, H. (2005) Effect of surface hydrophobicity on the adhesion of *S. cerevisiae* onto modified surfaces by poly (styrene-ran-sulfonic acid) random copolymers. *Colloids Surf B Biointerfaces* **46:** 70–77.

51. Kellis, M., Birren, B. W., and Lander, E. S. (2004) Proof and evolutionary analysis of ancient genome duplication in the yeast *Saccharomyces cerevisiae*. *Nature* **428:** 617–624.

52. Kim, K. H., Cho, Y. M., Kang, W. H., Kim, J. H., Byun, K. H., Park, Y. D., Bae, K. S., Park, H. M. (2001) Negative regulation of filamentous growth and flocculation by Lkh1, a fission yeast LAMMER kinase homolog. *Biochem Biophys Res Commun* **289**: 1237-1242.

53. Klis, F. M. (1994) Cell wall assembly in yeast. *Yeast* **10:** 851–869.

54. Klis, F. M., Boorsma, A., and De Groot, P. W. (2006) Cell wall construction in Saccharomyces cerevisiae. *Yeast* **23:** 185–202.

55. Klotz, S. A., Gaur, N. K., Lake, D. F., Chan, V., Rauceo, J., and Lipke, P. N. (2004) Degenerate peptide recognition by *Candida albicans* adhesins Als5p and Als1p. *Infect Immun* **72:** 2029–2034.

56. Kobayashi, O., Hayashi, N., Kuroki, R., and Sone, H. (1998) Region of Flo1 proteins responsible for sugar recognition. *J Bacteriol* **180:** 6503–6510.

57. Koelzer, S. and Klein, T. (2003) A Notch-independent function of Suppressor of Hairless during the development of the bristle sensory organ precursor cell of *Drosophila*. *Development* **130:** 1973-1988.

58. Kollar, R., Reinhold, B. B., Petrakova, E., Yeh, H. J., Ashwell, G., Drgonova, J., Kapteyn, J. C., Klis, F. M., and Cabib, E. (1997) Architecture of the yeast cell wall. Beta(1→6)-glucan interconnects mannoprotein, beta(1→3)-glucan, and chitin. *J Biol Chem* **272:** 17762–17775.

59. Kominami, K. and Toda, T. (1997) Fission yeast WD-repeat protein pop1 regulates genome ploidy through ubiquitin-proteasome-mediated degradation of the CDK inhibitor Rum1 and the S-phase initiator Cdc18. *Genes Dev* **11:** 1548-1560.

60. Kovall, R. A. and Hendrickson, W. A. (2004) Crystal structure of the nuclear effector of Notch signaling, CSL, bound to DNA. *EMBO J* **23:** 3441-3451.

61. Kovall, R. A. (2007) Structures of CSL, Notch and Mastermind proteins: piecing together an active transcription complex. *Curr Opin Struct Biol* **17:** 117-127.

62. Kron, S. J. (1997) Filamentous growth in budding yeast.*Trends Microbiol* **5:** 450–454.

63. Kussell, E. and Leibler, S. (2005) Phenotypic diversity, population growth, and information in fluctuating environments. *Science* **309:** 2075–2078.

64. Labbe, S., Pelletier, B., and Mercier, A. (2007) Iron homeostasis in the fission yeast *Schizosaccharomyces pombe*. *Biometals* **20:** 523-537.

65. Lai, E. C. (2002) Keeping a good pathway down: transcriptional repression of Notch pathway target genes by CSL proteins. *EMBO Rep* **3:** 840-845.

66. Lengeler, K. B., Davidson, R. C., D'Souza, C., Harashima, T., Shen, W. C., Wang, P., Pan, X., Waugh, M., and Heitman, J. (2000) Signal transduction cascades regulating fungal development and virulence. *Microbiol Mol Biol Rev* **64:** 746–785.

67. Linder, T. and Gustafsson, C. M. (2008) Molecular phylogenetics of ascomycotal adhesins – a novel family of putative cell-surface adhesive proteins in fission yeasts. *Fungal Genet Biol* **45:** 485-497.

68. Linder, T., Rasmussen, N. N., Samuelsen, C. O., Chatzidaki, E., Baraznenok, V., Beve, J., Henriksen, P., Gustafsson, C. M., and Holmberg, S. (2008) Two conserved modules of *Schizosaccharomyces pombe* Mediator regulate distinct cellular pathways. *Nucleic Acids Res* **36:** 2489-2504.

69. Lipke, P. N. and J. Kurjan. (1992) Sexual agglutination in budding yeasts: structure, function, and regulation of adhesion glycoproteins. *Microbiol Rev* **56:** 180–194.

70. Lipke, P. N. and R. Ovalle. (1998) Yeast cell walls: new structures, new challenges. *J Bacteriol* **180:** 3735–3740.

71. Liu, H. P. (2001) Transcriptional control of dimorphism in *Candida albicans*. *Curr Opin Microbiol* **4:** 728–735.

72. Livak, K. J. and Schmittgen, T. D. (2001) Analysis of relative gene expression data using real-time quantitative PCR and the 2(-Delta Delta C(T)) Method. *Methods* **25:** 402-408.

73. Madhani, H. and Fink, G. (1997) Combinatorial control required for the specificity of yeast MAPK signaling. *Science* **275:** 1314–1317.

74. Maidan, M. M., De Rop, L., Serneels, J., Exler, S., Rupp, S., Tournu, H., Thevelein, J. M., and Van Dijck, P. (2005) The G protein-coupled receptor Gpr1 and the G{alpha} protein Gpa2 act through the cAMP-protein kinase A pathway to induce morphogenesis in *Candida albicans*. *Mol Biol Cell* **16:** 1971–1986.

75. Masui, T., Long, Q., Beres, T. M., Magnuson, M. A., and MacDonald, R. J. (2007) Early pancreatic development requires the vertebrate Suppressor of Hairless (RBPJ) in the PTF1 bHLH complex. *Genes Dev* **21**: 2629-2643.

76. Mata, J. and Bahler, J. (2006) Global roles of Ste11p, cell type, and pheromone in the control of gene expression during early sexual differentiation in fission yeast. *Proc Natl Acad Sci USA* **103**: 15517–15522.

77. Matsunami, N., Hamaguchi, Y., Yamamoto, Y., Kuze, K., Kangawa, K., Matsuo, H., Kawaichi, M., and Honjo, T. (1989) A protein binding to the J kappa recombination sequence of immunoglobulin genes contains a sequence related to the integrase motif. *Nature* **342:** 934-937.

78. Mertins, P. and Gallwitz, D. (1987) A single intronless action gene in the fission yeast *Schizosaccharomyces pombe*: nucleotide sequence and transcripts formed in homologous and heterologous yeast. *Nucleic Acids Res* **15**: 7369-7379

79. Miki, B. L., Poon, N. H., James, A. P., and Seligy, V. L. (1982) Possible mechanism for flocculation interactions governed by gene FLO1 in *Saccharomyces cerevisiae*. *J Bacteriol* **150:** 878-889.

80. Miklos, I., Szilagyi, Z., Watt, S., Zilahi, E., Batta, G., Antunovics, Z., Enczi, K., Bahler, J., and Sipiczki, M. (2008) Genomic expression patterns in cell separation mutants of *Schizosaccharomyces pombe* defective in the genes sep10(+) and sep15(+) coding for the Mediator subunits Med31 and Med8. *Mol Genet Genomics* **279:** 225-238.

81. Minoguchi, S., Taniguchi, Y., Kato, H., Okazaki, T., Strobl, L. J., Zimber-Strobl, U., Bornkamm, G. W., and Honjo, T. (1997) RBP-L, a transcription factor related to RBP-Jkappa. *Mol Cell Biol* **17:** 2679-2687.

82. Morel, V. and Schweisguth, F. (2000) Repression by suppressor of hairless and activation by Notch are required to define a single row of single-minded expressing cells in the *Drosophila* embryo. *Genes Dev* **14:** 377-388.

83. Morita, T. and Takegawa, K. (2004) A simple and efficient procedure for transformation of *Schizosaccharomyces pombe*. *Yeast* **21:** 613-617.

84. Nguyen, B., Upadhyaya, A., van Oudenaarden, A., and Brenner, M. P. (2004) Elastic instability in growing yeast colonies. *Biophys J* **86:** 2740-2747.

85. Pan, X. W. and Heitman, J. (2000) Sok2 regulates yeast pseudohyphal differentiation via a transcription factor cascade that regulates cell-cell adhesion. *Mol Cell Biol* **20:** 8364–8372.

86. Pelletier, B., Beaudoin, J., Mukai, Y., and Labbe, S. (2002) Fep1, an iron sensor regulating iron transporter gene expression in *Schizosaccharomyces pombe*. *J Biol Chem* **277:** 22950-22958.

87. Převorovský, M., Půta, F., and Folk, P. (2007) Fungal CSL transcription factors. *BMC Genomics* **8:** 233.

88. Převorovský, M., Groušl, T., Staňurová, J., Ryneš, J., Nellen, W., Půta, F., and Folk, P. (2008) Cbf11 and Cbf12, the fission yeast CSL proteins, play opposing roles in cell adhesion and coordination of cell and nuclear division. *Exp Cell Res* **315**: 1533-1547.

89. Pursglove, S. E. and Mackay, J. P. (2005) CSL: a notch above the rest. *Int J Biochem Cell Biol* **37:** 2472-2477.

90. Reynolds, T. B. and Fink, G. R. (2001) Bakers' yeast, a model for fungal biofilm formation. *Science* **291:** 878-881.

91. Ribar, B., Banrevi, A., and Sipiczki, M. (1997) sep1+ encodes a transcription-factor homologue of the HNF-3/forkhead DNA-binding-domain family in *Schizosaccharomyces pombe*. *Gene* **202:** 1-5.

92. Rupp, S., Summers, E., Lo, H. J., Madhani, H., and Fink, G. (1999) MAP kinase and cAMP filamentation signaling pathways converge on the unusually large promoter of the yeast *FLO11* gene. *EMBO J* **18:** 1257–1269.

93. Rustici, G., van Bakel, H., Lackner, D. H., Holstege, F. C., Wijmenga, C., Bahler, J., and Brazma, A. (2007) Global transcriptional responses of fission and budding yeast to changes in copper and iron levels: a comparative study. *Genome Biol* **8:** R73.

94. Sampermans, S., Mortier, J., and Soares, E. V. (2005) Flocculation onset in *Saccharomyces cerevisiae*: the role of nutrients. *J Appl Microbiol* **98:** 525–531.

95. Samuelsen, C. O., Baraznenok, V., Khorosjutina, O., Spahr, H., Kieselbach, T., Holmberg, S., and Gustafsson, C. M. (2003) TRAP230/ARC240 and TRAP240/ARC250 Mediator subunits are functionally conserved through evolution. *Proc Natl Acad Sci USA* **100**: 6422–6427.

96. Sato, M., Maeba, H., Watari, J., and Takashio, M. (2002) Analysis of an inactivated Lg-*FLO1* gene present in bottom-fermenting yeast. *J Biosci Bioeng* **93:** 395–398.

97. Sharifmoghadam, M. R., Bustos-Sanmamed, P., Valdivieso, M. H. (2006) The fission yeast Map4 protein is a novel adhesin required for mating. *FEBS Lett* **580:** 4457–4462.

98. Shen, Z. M., Wang, L., Pike, J., Jue, C. K., Zhao, H., de Nobel, H., Kurjan, J., and Lipke, P. N. (2001) Delineation of functional regions within the subunits of the *Saccharomyces cerevisiae* cell adhesion molecule a-agglutinin. *J Biol Chem* **276:** 15768–15775.

99. Shirakata, Y., Shuman, J. D., and Coligan, J. E. (1996) Purification of a novel MHC class I element binding activity from thymus nuclear extracts reveals that thymic RBP-Jkappa/CBF1 binds to NF-kappaB-like elements. *J Immunol* **156:** 4672-4679.

100. Sipiczki, M., Grallert, B., and Miklos, I. (1993) Mycelial and syncytial growth in *Schizosaccharomyces pombe* induced by novel septation mutations. *J Cell Sci* **104 (Pt 2):** 485-493.

101. Stolz, J. (2003) Isolation and characterization of the plasma membrane biotin transporter from *Schizosaccharomyces pombe*. *Yeast* **20:** 221-231.

102. Stratford, M. (1992) Yeast flocculation – a new perspective. *Adv Microb Physiol* **33:** 1–71.

103. Straver, M. H., Kijne, J. W., and Smit, G. (1993) Cause and control of flocculation in yeast. *Trends Biotechnol* **11:** 228-232.

104. Szilagyi, Z., Grallert, A., Nemeth, N., and Sipiczki, M. (2002) The *Schizosaccharomyces pombe* genes sep10 and sep11 encode putative general transcriptional regulators involved in multiple cellular processes. *Mol Genet Genomics* **268:** 553-562.

105. Tanaka, N., Awai, A., Bhuiyan, M. S., Fujita, K., Fukui, H., and Takegawa, K. (1999) Cell surface galactosylation is essential for nonsexual flocculation in *Schizosaccharomyces pombe*. *J Bacteriol* **181:** 1356-1359.

106. Tang, Z., Mandel., L. L., Yean, S. L., Lin, C. X., Chen, T., Yanadiga, M., and Lin, R. J. (2003) The kic1 kinase of *Schizosaccharomyces pombe* is a CLK/STY orthologue that regulates cell-cell separation. *Exp Cell Res* **283**: 101–115.

107. Terrance, K., Heller, P., Wu, Y. S., and Lipke, P. N. (1987) Identification of glycoprotein components of alpha-agglutinin, a cell adhesion protein from *Saccharomyces cerevisiae*. *J Bacteriol* **169:** 475–482.

108. Tiede, A., Bastisch, I., Schubert, J., Orlean, P., and Schmidt, R. E. (1999) Biosynthesis of glycosylphosphatidylinositols in mammals and unicellular microbes. *Biol Chem* **380:** 503–523.

109. Tun, T., Hamaguchi, Y., Matsunami, N., Furukawa, T., Honjo, T., and Kawaichi, M. (1994) Recognition sequence of a highly conserved DNA binding protein RBP-J kappa. *Nucleic Acids Res* **22:** 965-971.

110. Udenfriend, S. and Kodukula, K. (1995) How glycosylphosphatidylinositol-anchored membrane proteins are made. *Annu Rev Biochem* **64:** 563–591.

111. Van Driessche, B., Tafforeau, L., Hentges, P., Carr, A. M., and Vandenhaute, J. (2005) Additional vectors for PCR-based gene tagging in *Saccharomyces cerevisiae* and *Schizosaccharomyces pombe* using nourseothricin resistance. *Yeast* **22:** 1061-1068.

112. Verstrepen, K. J., Reynolds, T. B., and Fink, G. R. (2004) Origins of variation in the fungal cell surface. *Nature Rev Microbiol* **2:** 533–540.

113. Verstrepen, K. J., Jansen, A., Lewitter, F., and Fink, G. R. (2005) Intragenic tandem repeats generate functional variability. *Nat Genet* **37:** 986–990.

114. Verstrepen, K. J. and Klis, F. M. (2006) Flocculation, adhesion and biofilm formation in yeasts. *Mol Microbiol* **60:** 5-15.

115. Vopálenská, I., Hůlková, M., Janderová, B., and Palková, Z. (2005) The morphology of *Saccharomyces cerevisiae* colonies is affected by cell adhesion and the budding pattern. *Res Microbiol* **156:** 921-931.

116. Voth, W. P., Olsen, A. E., Sbia, M., Freedman, K. H., and Stillman, D. J. (2005) ACE2, CBK1, and BUD4 in budding and cell separation. *Eukaryot Cell* **4:** 1018-1028.

117. Ward, M. P., Gimeno, C. J., Fink, G. R., and Garrett, S. (1995) SOK2 may regulate cyclic AMP-dependent protein kinase-stimulated growth and pseudohyphal development by repressing transcription. *Mol Cell Biol* **15:** 6854–6863.

118. Watson, P. and Davey, J. (1998) Characterization of the Prk1 protein kinase from *Schizosaccharomyces pombe*. *Yeast* **14:** 485-492.

119. Weinmaster, G. and Kintner, C. (2003) Modulation of Notch signaling during somitogenesis. *Annu Rev Cell Dev Biol* **19:** 367-395.

120. Wilson, J. J. and Kovall, R. A. (2006) Crystal structure of the CSL-Notch-Mastermind ternary complex bound to DNA. *Cell* **124:** 985-996.

121. Wojciechowicz, D., Lu, C.-F., Kurjan, J., and Lipke, P. N. (1993) Cell surface anchorage and ligand-binding domains of the *Saccharomyces cerevisiae* cell adhesion protein α-agglutinin, a member of the immunoglobulin superfamily. *Mol Cell Biol* **13:** 2554–2563.

122. Wood, V., Gwilliam, R., Rajandream, M. A., Lyne, M., Lyne, R., Stewart, A., Sgouros, J., Peat, N., Hayles, J., Baker, S., Basham, D., Bowman, S., Brooks, K., Brown, D., Brown, S., Chillingworth, T., Churcher, C., Collins, M., Connor, R., Cronin, A., Davis, P., Feltwell, T., Fraser, A., Gentles, S., Goble, A., Hamlin, N., Harris, D., Hidalgo, J., Hodgson, G., Holroyd, S., Hornsby, T., Howarth, S., Huckle, E. J., Hunt, S., Jagels, K., James, K., Jones, L., Jones, M., Leather, S., McDonald, S., McLean, J., Mooney, P., Moule, S., Mungall, K., Murphy, L., Niblett, D., Odell, C., Oliver, K., O'Neil, S., Pearson, D., Quail, M. A., Rabbinowitsch, E., Rutherford, K., Rutter, S., Saunders, D., Seeger, K., Sharp, S., Skelton, J., Simmonds, M., Squares, R., Squares, S., Stevens, K., Taylor, K., Taylor, R. G., Tivey, A., Walsh, S., Warren, T., Whitehead, S., Woodward, J., Volckaert, G., Aert, R., Robben, J., Grymonprez, B., Weltjens, I., Vanstreels, E., Rieger, M., Schafer, M., Muller-Auer, S., Gabel, C., Fuchs, M., Dusterhoft, A., Fritzc, C., Holzer, E., Moestl, D., Hilbert, H., Borzym, K., Langer, I., Beck, A., Lehrach, H., Reinhardt, R., Pohl, T. M., Eger, P., Zimmermann, W., Wedler, H., Wambutt, R., Purnelle, B., Goffeau, A., Cadieu, E., Dreano, S., Gloux, S., Lelaure, V., Mottier, S., Galibert, F., Aves, S. J., Xiang, Z., Hunt, C., Moore, K., Hurst, S. M., Lucas, M., Rochet, M., Gaillardin, C., Tallada, V. A., Garzon, A., Thode, G., Daga, R. R., Cruzado, L., Jimenez, J., Sanchez, M., del Rey, F., Benito, J., Dominguez, A., Revuelta, J. L., Moreno, S., Armstrong, J., Forsburg, S. L.,

Cerutti, L., Lowe, T., McCombie, W. R., Paulsen, I., Potashkin, J., Shpakovski, G. V., Ussery, D., Barrell, B. G., Nurse, P., and Cerrutti, L. (2002) The genome sequence of *Schizosaccharomyces pombe*. *Nature* **415:** 871-880.

123. Zhao, H., Chen, M. H., Shen, Z. M., Kahn, P. C., and Lipke, P. N. (2001) Environmentally induced reversible conformational switching in the yeast cell adhesion protein alpha-agglutinin. *Protein Sci* **10:** 1113–1123.

124. Zhou, S., Fujimuro, M., Hsieh, J. J., Chen, L., Miyamoto, A., Weinmaster, G., and Hayward, S. D. (2000) SKIP, a CBF1-associated protein, interacts with the ankyrin repeat domain of NotchIC To facilitate NotchIC function. *Mol Cell Biol* **20:** 2400-2410.

125. Zilahi, E., Miklos, I., and Sipiczki, M. (2000) The *Schizosaccharomyces pombe* sep15+ gene encodes a protein homologous to the Med8 subunit of the *Saccharomyces cerevisiae* transcriptional mediator complex. *Curr Genet* **38:** 227-232.

8 *APPENDICES*

8.1 Publications

Cbf11 and Cbf12, the fission yeast CSL proteins, play opposing roles in cell adhesion and coordination of cell and nuclear division

Martin Převorovský, Tomáš Groušl, Jana Staňurová, Jan Ryneš, Wolfgang Nellen, František Půta, Petr Folk

Experimental Cell Research, 2008

High environmental iron concentrations stimulate adhesion and invasive growth of *Schizosaccharomyces pombe*

Martin Převorovský, Jana Staňurová, František Půta, Petr Folk

FEMS Microbiology Letters, 2008